

2003-09

Final Report

Dynamic and Resilient Modulus of Mn/DOT Asphalt Mixtures



Research



Technical Report Documentation Page

| | | | |
|---|--|--|-----------|
| 1. Report No. MN/RC – 2003-09 | 2. | 3. Recipients Accession No. | |
| 4. Title and Subtitle DYNAMIC AND RESILIENT MODULUS OF MN/DOT ASPHALT MIXTURES | | 5. Report Date February 2003 | |
| | | 6. | |
| 7. Author(s) Timothy R. Clyne, Xinjun Li, Mihai O. Marasteanu, Eugene L. Skok | | 8. Performing Organization Report No. | |
| 9. Performing Organization Name and Address Department of Civil Engineering University of Minnesota 500 Pillsbury Dr. S.E. Minneapolis, MN 55455-0116 | | 10. Project/Task/Work Unit No. | |
| | | 11. Contract (C) or Grant (G) No. (c) 81655 (wo) 10 | |
| 12. Sponsoring Organization Name and Address Minnesota Department of Transportation Office of Research Services Mail Stop 330 395 John Ireland Boulevard St. Paul, Minnesota 55155 | | 13. Type of Report and Period Covered Final Report 2001-2003 | |
| | | 14. Sponsoring Agency Code | |
| 15. Supplementary Notes | | | |
| 16. Abstract (Limit: 200 words) <p>This report presents the results of laboratory testing to determine the complex modulus and phase angle of asphalt mixtures. Laboratory tests were performed on four different asphalt mixtures from the Mn/ROAD site. Testing was performed at six temperatures and five frequencies. Data from the tests were processed through a nonlinear regression curve fit to generate master curves of dynamic modulus and phase angle vs. frequency. These master curves were compared to results obtained from Witczak's predictive equations.</p> <p>It was found, as expected, that the dynamic modulus increased with an increase in frequency and a decrease in temperature. The model used to fit dynamic modulus master curves provided a good fit for the experimental data. The modulus values calculated using the 2000 predictive equation fit the test data reasonably well for Cell 21 and 35 mixtures, but the differences for Cells 33 and 34 were more significant. Smooth master curves for phase angle could not be obtained.</p> <p>An exploratory study to use a vibration exciter to measure dynamic modulus proved unsuccessful.</p> <p>This study was done under the framework of NCHRP Projects 1-37A, 9-19, and 9-29 that recommends dynamic modulus both as a design parameter and a simple performance test.</p> | | | |
| 17. Document Analysis/Descriptors Complex Dynamic Modulus Phase Angle Asphalt Mixtures Master Curve | | 18. Availability Statement No restrictions. Document available from: National Technical Information Services, Springfield, Virginia 22161 | |
| 19. Security Class (this report) Unclassified | 20. Security Class (this page) Unclassified | 21. No. of Pages 78 | 22. Price |

DYNAMIC and RESILIENT MODULUS of Mn/DOT ASPHALT MIXTURES

Final Report

Prepared by:

Timothy R. Clyne

Xinjun Li

Mihai O. Marasteanu

Eugene L. Skok

University of Minnesota
Department of Civil Engineering
500 Pillsbury Dr. S.E.
Minneapolis, MN 55455-0116

February 2003

Published by:

Minnesota Department of Transportation
Research Services
Mail Stop 330
395 John Ireland Boulevard
St. Paul, Minnesota 55155

This report represents the results of research conducted by the authors and does not necessarily represent the views or policy of the Minnesota Department of Transportation and/or the Center for Transportation Studies. This report does not contain a standard or specified technique.

ACKNOWLEDGEMENTS

The authors would like to thank Bruce Chadbourn, Shongtao Dai, Dave Van Deusen, and Glenn Engstrom at the Minnesota Department of Transportation (Mn/DOT) for their suggestions during the project. The authors would also like to thank Don Christensen, Ray Bonaquist, and Don Jack from Advanced Asphalt Technologies for providing information on modulus calculation and sample preparation protocol.

Table of Contents

| | |
|---|----|
| Chapter 1 Introduction | 1 |
| Background..... | 1 |
| Objectives | 1 |
| Scope..... | 1 |
| Report Organization..... | 2 |
| | |
| Chapter 2 Literature Review | 3 |
| History of Complex Modulus Testing | 3 |
| Superpave Shear Tester..... | 4 |
| Wave Methods | 5 |
| Linear Viscoelasticity Concepts | 5 |
| Master Curves and Shift Factors..... | 7 |
| Further Advances | 9 |
| Sample Preparation | 9 |
| Complex Modulus as a Design Parameter | 10 |
| Witczak Predictive Model..... | 10 |
| Complex Modulus as a Simple Performance Test..... | 11 |
| Fatigue Cracking..... | 12 |
| Rutting..... | 13 |
| Thermal Cracking | 13 |
| | |
| Chapter 3 Research Methodology | 15 |
| Materials | 15 |
| Testing Equipment | 16 |
| Sample Preparation | 17 |
| Testing Procedures..... | 18 |
| | |
| Chapter 4 Results and Discussion | 21 |

| | |
|---|-----------|
| Raw Data..... | 21 |
| Data Variables..... | 21 |
| Raw Data Plots..... | 22 |
| Data Analysis Method..... | 24 |
| Analysis of Test Data Results..... | 26 |
| Test Data..... | 26 |
| Comparison of Cell 35 Mixtures..... | 37 |
| Master Curves..... | 39 |
| Master Curves from the Test Data..... | 40 |
| Predictive Equations..... | 50 |
| Chapter 5 Vibration Testing..... | 57 |
| Introduction..... | 57 |
| Materials..... | 57 |
| Testing Equipment..... | 58 |
| Test Setup..... | 59 |
| Testing Procedures..... | 60 |
| Testing Results..... | 60 |
| Data Analysis..... | 61 |
| Chapter 6 Conclusions and Recommendations..... | 63 |
| Conclusions..... | 63 |
| Recommendations..... | 64 |
| References..... | 65 |

List of Tables

| | |
|---|----|
| Table 3.1. Material Properties..... | 15 |
| Table 3.2. Mixture Gradations..... | 15 |
| Table 3.3. Sample Preparation Data | 18 |
| Table 3.4. Cycles for Test Sequence..... | 19 |
| Table 4.1. Average Dynamic Modulus and Phase Angle for Cell 21..... | 27 |
| Table 4.2. Average Dynamic Modulus and Phase Angle for Cell 33..... | 28 |
| Table 4.3. Average Dynamic Modulus and Phase Angle for Cell 34..... | 29 |
| Table 4.4. Average Dynamic Modulus and Phase Angle for Cell 35 (Cored) | 30 |
| Table 4.5. Average Dynamic Modulus and Phase Angle for Cell 35 (Compacted)..... | 31 |
| Table 4.6. Dynamic Modulus Data Fit to Model..... | 41 |
| Table 4.7. Model Fit Parameters..... | 41 |
| Table 4.8. Cell 21 Dynamic Modulus from Witczak 1995 Model | 51 |
| Table 4.9. Cell 33 Dynamic Modulus from Witczak 1995 Model | 51 |
| Table 4.10. Cell 34 Dynamic Modulus from Witczak 1995 Model | 51 |
| Table 4.11. Cell 35 (cored) Dynamic Modulus from Witczak 1995 Model..... | 52 |
| Table 4.12. Cell 21 Dynamic Modulus from Witczak 2000 Model | 52 |
| Table 4.13. Cell 33 Dynamic Modulus from Witczak 2000 Model | 52 |
| Table 4.14. Cell 34 Dynamic Modulus from Witczak 2000 Model | 52 |
| Table 4.15. Cell 35 (cored) Dynamic Modulus from Witczak 2000 Model..... | 53 |
| Table 5.1. Material Properties..... | 57 |
| Table 5.2. Mixture Gradations..... | 57 |
| Table 5.3. Sample Preparation Data | 58 |

List of Figures

| | |
|--|----|
| Figure 2.1. Complex Modulus Concepts | 6 |
| Figure 2.2. Example of a Complex Modulus Master Curve | 8 |
| Figure 3.1. Dynamic Modulus Test Setup | 16 |
| Figure 4.1. Typical Force, Displacement vs. Time Plot at Low Temperature (-20°C) | 23 |
| Figure 4.2. Typical Force, Displacement vs. Time Plot at High Temperature (40°C) | 23 |
| Figure 4.3. Dynamic Modulus vs. Frequency for Cell 21 | 32 |
| Figure 4.4. Phase Angle vs. Frequency for Cell 21 | 32 |
| Figure 4.5. Dynamic Modulus vs. Frequency for Cell 33 | 33 |
| Figure 4.6. Phase Angle vs. Frequency for Cell 33 | 33 |
| Figure 4.7. Dynamic Modulus vs. Frequency for Cell 34 | 34 |
| Figure 4.8. Phase Angle vs. Frequency for Cell 34 | 34 |
| Figure 4.9. Dynamic Modulus vs. Frequency for Cell 35 (Cored) | 35 |
| Figure 4.10. Phase Angle vs. Frequency for Cell 35 (Cored) | 35 |
| Figure 4.11. Dynamic Modulus vs. Frequency for Cell 35 (Compacted) | 36 |
| Figure 4.12. Phase Angle vs. Frequency for Cell 35 (Compacted) | 36 |
| Figure 4.13. Dynamic Modulus Comparison for Cell 35 | 38 |
| Figure 4.14. Phase Angle Comparison for Cell 35 | 39 |
| Figure 4.15. Dynamic Modulus Master Curves | 42 |
| Figure 4.16. Dynamic Modulus Master Curve for Cell 21 | 43 |
| Figure 4.17. Dynamic Modulus Master Curve for Cell 33 | 43 |
| Figure 4.18. Dynamic Modulus Master Curve for Cell 34 | 44 |
| Figure 4.19. Dynamic Modulus Master Curve for Cell 35 (cored) | 44 |
| Figure 4.20. Dynamic Modulus Master Curve for Cell 35 (compacted) | 45 |
| Figure 4.21. Shift Factor vs. Temperature | 45 |
| Figure 4.22. Dynamic Modulus vs. Temperature at 10 Hz | 47 |
| Figure 4.23. Phase Angle Master Curve for Cell 21 | 48 |
| Figure 4.24. Phase Angle Master Curve for Cell 33 | 48 |
| Figure 4.25. Phase Angle Master Curve for Cell 34 | 49 |
| Figure 4.26. Phase Angle Master Curve for Cell 35 | 49 |

| | |
|---|----|
| Figure 4.27. Master Curve Comparison (Cell 21) | 53 |
| Figure 4.28. Master Curve Comparison (Cell 33) | 54 |
| Figure 4.29. Master Curve Comparison (Cell 34) | 54 |
| Figure 4.30. Master Curve Comparison (Cell 35) | 55 |
| Figure 5.1. Vibration Exciter Type 4809 | 58 |
| Figure 5.2. Vibration Test Setup..... | 59 |
| Figure 5.3. Vibration Test Results for Sample 58-40-1 | 60 |
| Figure 5.4. Vibration Test Results for Sample 58-40-4..... | 61 |

EXECUTIVE SUMMARY

The 2002 Design Guide proposes the use of the complex modulus of asphalt mixtures as a parameter in the design procedure. The complex modulus also emerged as a lead candidate for a Simple Performance Test to predict rutting and fatigue cracking in asphalt pavements. Therefore, it becomes an important priority to accurately determine the complex modulus of asphalt mixtures over a wide range of temperatures and frequencies. An equation was proposed in the design guide to predict dynamic modulus values using asphalt mixture components properties; its validity needs to be proven for typical asphalt mixtures used in Minnesota. In addition, comparison of the laboratory data with existing field data collected from the Minnesota Road Research Project (Mn/ROAD) can be used to further investigate the role of the complex modulus of asphalt mixtures in predicting the performance of flexible pavements.

Asphalt mixtures from four cells at Mn/ROAD were analyzed in this study: Cells 21, 33, 34, and 35. The latter three mixtures had identical mix designs except for the asphalt type (PG 58-28, PG 58-34, and PG 58-40, respectively), while the Cell 21 mixture contains Pen 120/150 asphalt and was cored from the existing pavement. In addition, the Cell 35 mixture (PG 58-40) was chosen to evaluate two different sample preparation techniques and their effect on the complex modulus magnitude.

The absolute value of the complex modulus and the phase angle were measured at temperatures of -20, -10, 4, 20, 40, and 54°C and frequencies of 25, 10, 1, 0.1, and 0.01 Hz. Sample preparation, test procedures, and data analysis followed the recommendations proposed in the National Cooperative Highway Research Program (NCHRP) 9-29. In addition, a preliminary investigation explored the possibility of measuring the complex modulus of asphalt mixtures using a less expensive vibration testing device.

The raw test data was manipulated to obtain modulus and phase angle values for each combination of temperature and frequency. Complex modulus master curves were constructed for each mixture using nonlinear regression techniques to fit the experimental data to a sigmoidal function using the following equation:

$$\log|E^*| = \delta + \frac{\alpha}{1 + e^{\beta - \gamma(\log(f_r) + sT)}}$$

where δ , α , β and γ are fit constants, f_T is the test frequency, and s_T is the shift factor for each temperature. Smooth master curves could not be constructed for the phase angle.

The dynamic modulus for each mixture also was calculated using two predictive equations developed as part of the 2002 Design Guide. The predicted values were compared to the laboratory test results. The 2000 predictive equation fit the data for Cells 21 and 35 reasonably well, but not for Cells 33 and 34.

The limited data obtained in this project showed that the sample preparation method has a significant effect on the modulus results. The proposed procedure of compacting large specimens, coring, and cutting to obtain test specimens should be followed. The limited experiment performed in this project showed that the dynamic complex modulus values obtained with the vibration method are not reliable.

Recommendations for further study include testing more asphalt mixtures to encompass a wider range of materials used in Minnesota, correlating complex modulus results to other tests performed on mixtures, and improving the use of a vibration device to accurately measure complex modulus.

Chapter 1

Introduction

Background

The National Cooperative Highway Research Program (NCHRP) Project 1-37A (Development of the *2002 Guide for the Design of New and Rehabilitated Pavement Structures: Part II*) is responsible for developing the *2002 Guide for the Design of Pavement Structures*. This guide recommends using the complex modulus as a design parameter in the mechanistic design procedure. NCHRP Projects 9-19 (Superpave Support and Performance Models Management) and 9-29 (Simple Performance Tester for Superpave Mix Design) document the development of a Simple Performance Test for evaluating the resistance of asphalt mixtures to permanent deformation and fatigue cracking. The complex modulus test is the most promising test for both of these distress predictions. Therefore it is necessary to accurately determine the complex modulus of asphalt mixtures over a wide range of temperatures and frequencies.

Objectives

The main objective of this project was to perform complex modulus tests on four typical Minnesota asphalt mixtures and generate master curves of modulus vs. frequency from the test data. The experimental master curves were compared against modulus values obtained from two predictive equations proposed by 2002 Design Guide. A small study that investigated the effects of sample preparation techniques on complex modulus was undertaken. In addition, a preliminary investigation explored the possibility of measuring the complex modulus of asphalt mixtures using a less expensive vibration testing device.

Scope

Four different asphalt mixtures from the Minnesota Road Research Project (Mn/ROAD) were evaluated in this study. Three cells contained mixtures with exactly the same mix design except for asphalt type (PG 58-28, PG 58-34, and PG 58-40). The fourth cell had a different mix design and asphalt type (120/150). In addition, the Cell 35 mixture (PG 58-40) was chosen to evaluate two different sample preparation techniques and their effect on dynamic modulus. The

dynamic modulus and phase angle were measured at temperatures of -20, -10, 4, 20, 40, and 54°C and frequencies of 25, 10, 1, 0.1, and 0.01 Hz. Sample preparation, test procedures, and data analysis followed the recommendations in NCHRP 9-29.

Report Organization

This report is arranged into six sections: Introduction, Literature Review, Research Methodology, Results and Discussion, Vibration Testing, and Conclusions and Recommendations. The Literature Review provides a background of complex modulus testing procedures, linear viscoelasticity concepts, and sample preparation in relation to the use of complex modulus as a design parameter and simple performance test. Research Methodology discusses the asphalt mixtures, testing equipment, sample preparation procedures, and dynamic modulus test methods. Results and Discussion describes the raw data obtained, data analysis methods, master curve generation, and comparisons with predictive equations. The Vibration Testing chapter describes the procedure and reports vibration test results. The report closes with some final conclusions and recommendations. The references include citations for literature sources used as supporting materials.

Chapter 2

Literature Review

History of Complex Modulus Testing

Complex modulus testing for asphalt mixtures is not a new concept. In 1962, Papazian was one of the first to describe viscoelastic tests performed on asphalt mixtures [1]. He applied a sinusoidal stress to a cylindrical specimen at a given frequency and measured a sinusoidal strain response at the same frequency. Tests were conducted under controlled temperature conditions at varying load amplitudes and frequencies. He concluded that viscoelastic concepts could be applied to asphalt pavement design and performance. Forty years after these experiments, we still are using these concepts to develop mix design criteria and evaluate the performance of the material on the road.

Work continued in the next decade that considered compression, tension, and tension-compression loading. A number of studies indicated differences in $|E^*|$ obtained from different loading conditions. The differences affect especially the phase angle and tend to become more significant at higher test temperatures. Witczak and Root indicate that the tension-compression test may be more representative to field loading conditions [2]. Khanal and Mamlouk affirm this assertion [3]. They performed complex modulus tests under five different modes of loading and obtained different results, especially at high temperatures. By using a bimodular analysis technique, including the modulus found both in tension and compression, they were able to better predict asphalt concrete behavior under field loading conditions. Bonnaure et al. determined the complex modulus from a bending test [4]. In this test a trapezoidal specimen fixed at the bottom is subjected to a sinusoidal load at the free end. The deformation is measured, and the complex modulus is calculated from the results.

In the late 1980s and early 1990s the International Union of Testing and Research Laboratories for Materials and Structures (RILEM) Technical Committee on Bitumen and Asphalt Testing organized an international testing program [5]. The goal of the program was to promote and develop mix design methodologies and associated significant measuring methods for asphalt pavements. Complex modulus tests were performed by 15 participating laboratories in countries throughout Europe. Measurements were made at various temperatures and

frequencies, and each laboratory used different specimen shape, testing geometry, and loading conditions. Depending on the facility, complex modulus and/or phase angle were reported. Results showed that bending tests and indirect tension tests were in reasonable agreement under certain conditions. The laboratories were able to reproduce the phase angle ϕ much better than the modulus absolute value $|E^*|$.

Work continued in the 1990s with the construction of Mn/ROAD. Complex modulus tests were performed on both tall cylindrical specimens and indirect tensile specimens [6], [7], [8]. The study revealed mixed results, showing that tests on the same material with the two different setups sometimes yielded different results for the dynamic modulus and phase angle. The phase angle was especially variable in both test setups. The study included a comprehensive discussion of diametral loading, which documented the viscoelastic behavior of asphalt concrete under haversine loading.

The most comprehensive research effort started in the mid-1990s as part of the NCHRP projects mentioned above. This research proposed new guidelines for the proper specimen geometry and size, specimen preparation, testing procedure, loading pattern, and empirical modeling. In these two projects the terminology was changed to dynamic complex modulus.

Superpave Shear Tester

In addition to the traditional means of complex modulus testing mentioned above, the modulus also can be obtained from the Superpave Shear Tester (SST), a device used for the Repeated Shear at Constant Height Test (RSCH). The SST is a servo-hydraulic machine capable of applying controlled vertical and horizontal loads to a specimen 150 mm in diameter and 50 mm tall. The RSCH test (AASHTO TP7-94) consists of applying 5,000 cycles of a 0.1-second shear load pulse followed by a 0.6-second rest period. The axial load is varied automatically to maintain a constant specimen height. The permanent shear deformation of the specimen after 5,000 load cycles is recorded and used in performance predictions.

Results from the Superpave Shear Tester have been shown to relate to rutting performance. Therefore, the SST is considered a candidate for the Simple Performance Test being developed under NCHRP Projects 9-19 and 9-29. One major drawback of this test method is that data from RSCH tests are highly variable. Even the generally accepted sample air void range of ± 0.5 percent may need to be reduced to lower the variation. Several steps have been

taken to attempt to minimize testing variation, such as increasing the number of samples, using additional LVDTs, and various statistical analysis procedures [9].

Wave Methods

Another approach to obtaining the dynamic modulus of asphalt mixtures involves the use of wave propagation techniques. Blaine and Burlot [10] made measurements on a test pavement with the light Goodman vibrator. This method consisted of a rod that vibrated at frequencies between 20 to 20,000 Hz and at temperatures between 0° and 40°C. Dispersion curves were constructed, plotting the wave velocity vs. wavelength. The Rayleigh speed of the asphalt mixture was obtained by extrapolating the curve to where the wavelength is equal to zero. The Rayleigh wave speed then was related to the complex modulus of the material. Poisson's ratio of the material and the mixture temperature affected on the results of the complex modulus testing in this fashion.

Dos Reis et al. have presented a modified version of the impulse-echo method as a means to non-destructively estimate the dynamic complex modulus and other material characteristics [11]. By using principles of statistical energy analyses, they proposed a method based on the energy-density decay function of a diffuse wave field to determine an “optimum microstructure” for asphalt concrete.

Hochuli et al. also used wave methods to determine the complex modulus of asphalt mixtures [12]. Their research involved generating flexural waves in an asphalt concrete rod to determine $|E^*|$ for various frequencies. They recognize the complexity of using wave propagation because of the inhomogeneities and extreme temperature dependence of asphalt. Wave propagation is described as a promising non-destructive test method with the potential of in situ measurements for the continuous determination of the complex modulus of asphalt mixtures.

Linear Viscoelasticity Concepts

The evaluation of complex modulus tests requires an understanding of linear viscoelasticity concepts. Ferry [13] describes the fundamental concepts of linear viscoelasticity. For the one-dimensional case of a sinusoidal loading, the following equation can represent the stress:

$$\sigma = \sigma_o \cdot \sin(\omega t) \quad (2.1)$$

In equation (2.1) σ_o is the stress amplitude and ω is the angular velocity, which is related to the frequency f by:

$$\omega = 2\pi f \quad (2.2)$$

The resulting steady state strain can be written as:

$$\varepsilon = \varepsilon_o \cdot \sin(\omega t - \delta) \quad (2.3)$$

in which ε_o is the strain amplitude and δ is the phase angle related to the time the strain lags the stress, as shown in Figure 2.1. Phase angle is an indicator of the viscous (or elastic) properties of the material. For a pure elastic material, $\delta = 0^\circ$, and for a pure viscous material, $\delta = 90^\circ$.

The ratio of the stress to strain amplitudes defines the absolute value of the dynamic modulus. The in-phase and out-of phase components are used to define the storage modulus:

$$E' = \frac{\sigma_o \cos(\delta)}{\varepsilon_o} \quad (2.4)$$

and the loss modulus:

$$E'' = \frac{\sigma_o \sin(\delta)}{\varepsilon_o} \quad (2.5)$$

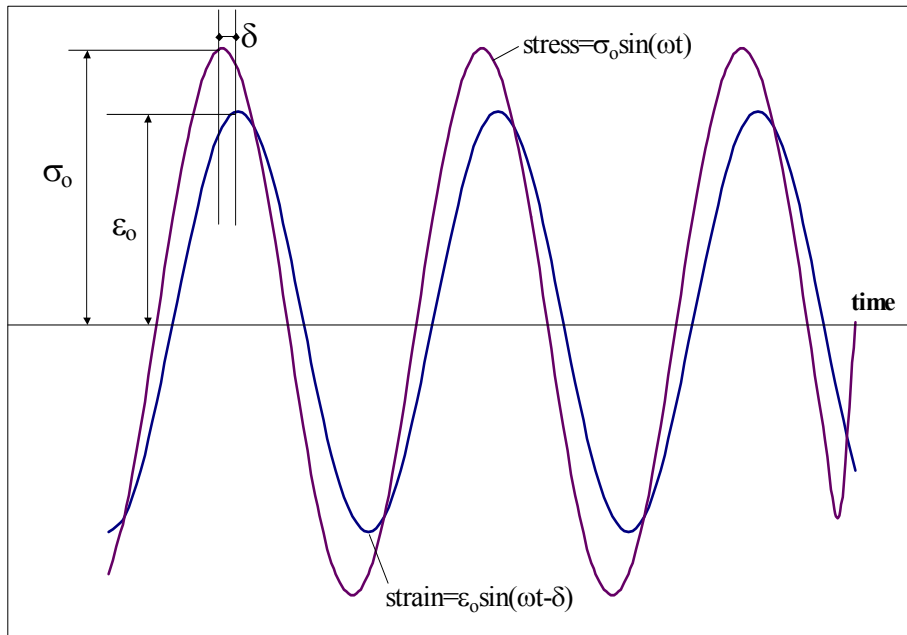


Figure 2.1. Stress and Strain in Dynamic Loading

A simplification of the preceding calculations is achieved by expressing the stress and strain in complex form:

$$\sigma^* = \sigma_o e^{i\omega t} \quad (2.6)$$

and the resulting strain:

$$\varepsilon^* = \varepsilon_o e^{i(\omega t - \delta)} \quad (2.7)$$

From equations (2.6) and (2.7) the complex modulus, $E^*(i\omega)$, is defined as the complex quantity:

$$E^*(i\omega) = \frac{\sigma^*}{\varepsilon^*} = \frac{\sigma_o}{\varepsilon_o} e^{i\delta} = E' + iE'' \quad (2.8)$$

The real part of the complex modulus is the storage modulus and the imaginary part is the loss modulus. The dynamic complex modulus is the absolute value of the complex modulus:

$$|E^*| = \frac{\sigma_o}{\varepsilon_o} \quad (2.9)$$

Master Curves and Shift Factors

Analysis of complex modulus test data often involves generating master curves. The master curve of an asphalt mixture allows comparisons to be made over extended ranges of frequencies or temperatures. Master curves are generated using the time-temperature superposition principle. This principle allows for test data collected at different temperatures and frequencies to be shifted horizontally relative to a reference temperature or frequency, thereby aligning the various curves to form a single master curve. Figure 2.2 shows a sample master curve of an asphalt mixture obtained in this project.

The shift factor, $\alpha(T)$, defines the required shift at a given temperature. The actual frequency is divided by this shift factor to get a reduced frequency, f_r , for the master curve:

$$f_r = \frac{f}{\alpha(T)} \quad \text{or} \quad \log(f_r) = \log(f) - \log[\alpha(T)] \quad (2.10)$$

The master curve for a material can be constructed using an arbitrarily selected reference temperature, T_R , to which all data are shifted. At the reference temperature, the shift factor $\alpha(T) = 1$. Several different models have been used to obtain shift factors of viscoelastic materials, the most common of which is the Williams-Landel-Ferry (WLF) equation [14].

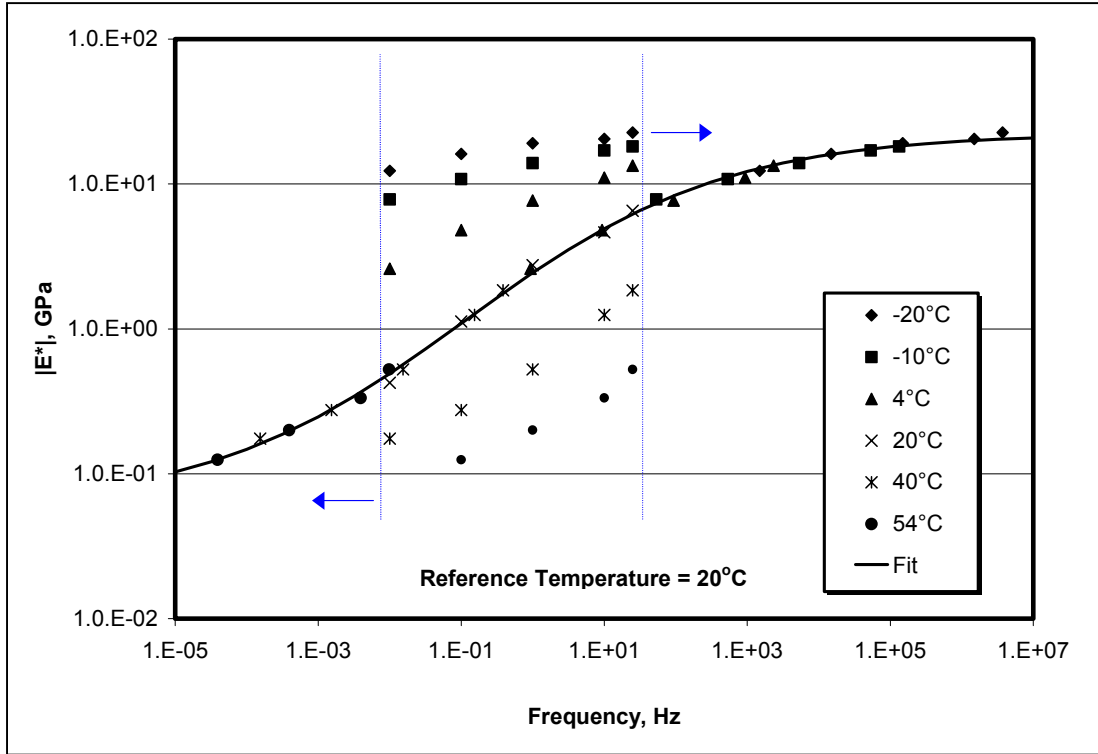


Figure 2.2. Example of a Complex Modulus Master Curve

When experimental data is available, a master curve can be constructed for the mixture. The master curve can be represented by a nonlinear sigmoidal function of the following form [15]:

$$\log|E^*| = \delta + \frac{\alpha}{1 + e^{\beta + \gamma(\log(t_r))}} \quad (2.11)$$

In equation (2.11) t_r is the time of loading at the reference temperature, δ is the minimum value of $|E^*|$, $\delta + \alpha$ is the maximum value of $|E^*|$, and β and γ are parameters describing the shape of the sigmoidal function. Note that δ in this equation is not related to the phase angle; it is just the notation chosen by University of Arizona research team for the minimum modulus value. The sigmoidal function of the dynamic modulus master curve can be justified by physical observations of the mixture behavior. The upper part of the function approaches asymptotically the mix's maximum stiffness, which depends on the binder stiffness at cold temperatures. At high temperatures, the compressive loading causes aggregate interlock stiffness to be an indicator of mixture stiffness. The sigmoidal function presented in equation (2.11) captures the

physical behavior of asphalt mixtures observed in complex modulus testing throughout the entire temperature range [16].

Further Advances

Daniel et al. [17] report on work that they have done to consider the effects of aging on viscoelastic materials. They focused on how the fatigue performance of asphalt mixtures, which relates to viscoelastic material properties, changes with time because of changing material properties. Their approach involved subjecting asphalt mixtures to certain aging conditions and measuring the physical properties of the aged mixture via uniaxial complex modulus and tensile creep and recovery tests. The researchers advanced an existing uniaxial constitutive model developed by Lee and Kim [18]. This model employs the elastic-viscoelastic correspondence principle and damage parameter based on Schapery's work-potential theory to model the stress-strain behavior of asphalt mixtures subject to cyclic loading. Daniel et al. [17] successfully established an analytical and experimental methodology for incorporating the effects of aging in the current constitutive model.

In addition, Pellinen and Witczak [16] developed a method for constructing stress-dependent master curves using complex modulus test data. The method uses a non-linear elasticity model to incorporate stress dependency into the master curve. This stress dependency is included in the equilibrium modulus value of the master curve, rather than incorporating it into the shift factors. The stress dependency and non-linearity are considered only at intermediate and high temperatures, and the model assumes linear viscoelastic material behavior at cold temperatures.

Sample Preparation

Currently, there is much discussion about the shape and size of specimen to be used in complex modulus testing. In Europe researchers have experimented with a number of different testing geometries [5], while in the United States researchers generally have tested either tall cylinders under uniaxial or triaxial loading [1] or short cylinders under indirect tensile loading [7], [8]. In NCHRP Project 9-19 Witczak and his colleagues investigated the proper size and geometry of test specimens [19]. They designed full factorial experiments using nominal maximum aggregate size, aspect ratio, and diameter as the controlled variables. The results were

analyzed using ANOVA and graphical techniques. Another consideration was the repeatability of test results. Based on numerous complex modulus test results, they recommended using 100-mm diameter cored specimens from a 150-mm diameter gyratory compacted specimen, with a final cut (sawed) height of 150 mm. Fully lubricated end plates (by use of Teflon paper or other methods) were found to minimize end restraint to the specimen. Increasing the number of gages used to measure axial strain decreases the number of test specimens necessary.

This recommendation came from a study by Chehab et al. [20] that considered the variation in air voids within specimens compacted using the Superpave Gyratory Compactor (SGC). The study showed that specimens compacted using the SGC tend to have non-uniform air void distribution both along their diameter and height. SGC-compacted specimens have higher air void content at the top and bottom edges, as well as sections adjacent to the mold walls, than the interior portion of the specimens have.

Complex Modulus as a Design Parameter

As previously mentioned, the *2002 Guide for the Design of Pavement Structures* recommends the dynamic complex modulus as a design parameter in their mechanistic-empirical design procedure [15]. Level 1 Analysis requires actual dynamic modulus test data to develop master curves and shift factors based on equations (2.10) and (2.11). This testing is performed on replicate samples at five temperatures and four rates of loading per temperature. Binder testing also must be done at this level to shift the data into smooth master curves. Level 2 Analysis constructs a master curve using actual asphalt binder test data based on the relationship between binder viscosity and temperature. Level 3 Analysis requires no laboratory test data. Instead the Witczak modulus equation [15] is used with typical temperature-viscosity relationships established for all binder grades.

Witczak Predictive Model

In lieu of actual complex modulus test data, Witczak and Fonseca propose an empirical model to predict the complex modulus of an asphalt mixture. The proposed model for complex modulus master curves was generated based on a large amount of data consisting of 1,429 points from 149 separate asphalt mixtures. Improvements were made to earlier models, taking into account hardening effects from short- and long-term aging, as well as extreme temperature

conditions. Based on the gradation of aggregates in the mixture and asphalt binder properties, the final dynamic modulus model developed from this statistical study was [21]:

$$\log|E^*| = -0.261 + 0.008225 P_{200} - 0.0000101 (P_{200})^2 + 0.00196 P_4 - 0.03157 V_a - 0.415 \frac{V_{beff}}{(V_{beff} + V_a)} + \frac{[1.87 + 0.002808 P_4 + 0.00000404 P_{38} - 0.0001786 (P_{38})^2 + 0.0164 P_{34}]}{1 + e^{(-0.716 \log f - 0.7425 \log \eta)}} \quad (2.12)$$

where

$|E^*|$ = asphalt mix complex modulus, in 10^5 psi;

η = bitumen viscosity, in 10^6 poise;

f = load frequency, in Hz;

V_a = percent air voids in the mix, by volume;

V_{beff} = percent effective bitumen content, by volume;

P_{34} = percent retained on $\frac{3}{4}$ -in. sieve, by total aggregate weight (cumulative);

P_{38} = percent retained on $\frac{3}{8}$ -in. sieve, by total aggregate weight (cumulative);

P_4 = percent retained on No. 4 sieve, by total aggregate weight (cumulative); and

P_{200} = percent passing No. 200 sieve, by total aggregate weight.

With the accumulation of more and more test data, Dr. Witczak developed a new predictive equation for the dynamic modulus based on equation (2.12). The new model is shown in equation (2.13).

$$\log|E^*| = -1.249937 + 0.029232 P_{200} - 0.001767 (P_{200})^2 + 0.002841 P_4 - 0.058097 V_a - 0.802208 \frac{V_{beff}}{(V_{beff} + V_a)} + \frac{[3.871977 - 0.0021 P_4 + 0.003958 P_{38} - 0.000017 (P_{38})^2 + 0.00547 P_{34}]}{1 + e^{(-0.603313 - 0.313351 \log f - 0.393532 \log \eta)}} \quad (2.13)$$

This equation uses the same parameters as equation (2.12). There was no change in the form of the equation, although all the constant coefficients were changed to reflect calibration to more data [15].

Complex Modulus as a Simple Performance Test

The goal of NCHRP Project 9-19 was to develop a Simple Performance Test (SPT) for asphalt mixtures. Various testing configurations were evaluated from several of the most

promising test methods. The potential SPT methods can be categorized as stiffness-related tests, deformability tests, and cracking tests. The stiffness parameters were obtained from compressive complex modulus, Simple Shear Tester (SST), and ultrasonic wave propagation. Of these three candidates, the complex dynamic modulus appeared to be the most promising for relating material properties (namely, stiffness) to rutting and fatigue cracking observed in the field [22].

Fatigue Cracking

Witczak et al. performed numerous complex modulus tests to perfect the recommendations for fatigue cracking in asphalt mixtures [23]. They performed tests on specimens fabricated following the recommendations previously mentioned. The test results led to the development of a fatigue distress model in which the number of repetitions to failure, N_f , is a function of horizontal tensile strain, ε_t , which represents the largest of the transverse and longitudinal horizontal strain, and dynamic modulus of the mix, $|E^*|$:

$$N_f = FK_{1\alpha} \left(\frac{1}{\varepsilon_t} \right)^5 \left(\frac{1}{|E^*|} \right)^{1.4} \quad (2.14)$$

The adjustment factor, F , that indicates the stress or strain controlled fatigue behavior in the pavement structure, is a function of the dynamic modulus and pavement thickness, h_{ac} :

$$F = 1 + \frac{13909 \cdot |E^*|^{-0.4} - 1}{1 + e^{(1.354 \cdot h_{ac} - 5.408)}} \quad (2.15)$$

A volumetric adjustment factor, $K_{1\alpha}$, corrects the number of repetitions to failure by taking into account the binder and mix properties. In the following equation, PI is the binder penetration index and V_b is the volume of binder in the mix.

$$K_{1\alpha} = [0.0252 \cdot PI - 0.00126 \cdot PI(V_b) + 0.00673 \cdot V_b - 0.0167]^5 \quad (2.16)$$

Equation (2.14) can be reduced to the following equation, where the constants β_n and k_n can be assigned to nationally calibrated fatigue model constants:

$$N_f = \beta_{f1} k_1 \left(\frac{1}{\varepsilon_t} \right)^{\beta_{f2} k_2} \left(\frac{1}{|E^*|} \right)^{\beta_{f3} k_3} \quad (2.17)$$

The complex modulus test has the potential to relate the Superpave volumetric mix design directly to the structural field performance through the *2002 Guide for the Design of*

Pavement Structures. The parameters found through this research will be studied further and will result in the final recommended Simple Performance Test for fatigue cracking in the 2002 Design Guide.

Rutting

The complex modulus test also showed good correlation to permanent deformation (rutting) of asphalt mixtures. Witczak et al. [24] performed research on asphalt mixtures similar to the SPT for fatigue cracking. Cylindrical specimens were tested at five temperatures and six frequencies, as well as different levels of confining pressure. They came to preliminary findings that warranted a closer look at the dynamic modulus test for rutting susceptibility. Pellinen and Witczak [22] recommend using $|E^*|$ obtained in unconfined compression at 54.4°C and a frequency of 5 Hz. The stress levels must remain small to keep the sample in the linear viscoelastic region. Some other recommendations from this project include [24]:

- Prediction of one-dimensional densification, as well as lateral displacement of the mix and tertiary flow.
- Inclusion of temperature as a key factor for permanent deformation modeling.
- Inclusion of HMA layer thickness and total HMA thickness.
- Consideration of pavement type and rehabilitation strategy.

Thermal Cracking

Recent research by Pellinen and Witczak [22] showed that the complex modulus of asphalt mixtures was not a good performance indicator for thermal cracking, although they encouraged further study. Additional research by Witczak et al. [23] proposed a method to characterize the asphalt material using the creep compliance master curve and relaxation modulus to incorporate the linear viscoelastic nature of the asphalt mix behavior to pavement response models. Based on linear viscoelasticity, the complex modulus was transformed into creep compliance values. Eventually a model was developed using fracture mechanics that related the computed crack depth to crack frequency. While this approach arrived at a model relating complex modulus values to thermal cracking in the pavement, it also required creep compliance and indirect tensile tests to complete the prediction. This thermal cracking model

will be studied further under NCHRP Project 9-29 currently under way, and a final recommended Simple Performance Test will result.

Chapter 3

Research Methodology

Materials

The focus of this research was to evaluate the complex modulus of several asphalt mixtures from Mn/ROAD. Four different mixtures were selected at the beginning of the project and tested. Basic properties of the mixtures are shown in Table 3.1. The mixture gradations are found in Table 3.2. Cells 33, 34, and 35 have identical mixture properties, except for the binder type, which allows the investigation of the effect of binder type on the complex modulus of asphalt mixtures.

Table 3.1. Material Properties

| Cell | 21 | 33 | 34 | 35 |
|--------------------------|-----------|-------------|-------------|-------------|
| Binder Type | 120/150 | PG 58-28 | PG 58-34 | PG 58-40 |
| Polymer Modified? | No | No | Yes | Yes |
| Sample Type | Core | Loose Mix | Loose Mix | Loose Mix |
| Paving Date | July 1993 | August 1999 | August 1999 | August 1999 |

Table 3.2. Mixture Gradations

| Sieve Size, mm | Sieve Size, in. | Percent Passing | | | |
|----------------|-----------------|-----------------|---------|---------|---------|
| | | Cell 21 | Cell 33 | Cell 34 | Cell 35 |
| 19 | 3/4 | 100 | 100 | 100 | 100 |
| 16 | 5/8 | 99 | | | |
| 12.5 | 1/2 | 96 | 94 | 94 | 94 |
| 9.0 | 3/8 | 88 | 86 | 86 | 86 |
| 4.75 | #4 | 70 | 66 | 66 | 66 |
| 2.36 | #8 | | 54 | 54 | 54 |
| 2.0 | #10 | 58 | | | |
| 1.0 | #20 | 44 | | | |
| 0.45 | #40 | 26 | | | |
| 0.25 | #80 | 9 | | | |
| 0.075 | #200 | 4.3 | 4.7 | 4.7 | 4.7 |

Testing Equipment

All tests were performed on an MTS 810.22 servo-hydraulic testing system, which includes an MTS 318.10 Load Frame, rated at 100 kN, with integrally mounted 150 mm stroke actuator, position transducer, and load cell. The TestStar IIs control system was used to set up and perform the tests and to collect the data. The software package MultiPurpose TestWare was used to custom design the tests and collect the raw test data.

Flat, circular load platens were used to apply the load to the specimen. Teflon paper was used to reduce friction at the end plates. The vertical deformation measurements were obtained using two MTS 632.94 E-20 extensometers with a 114-mm gage length. They were attached to the specimen by springs, along with a drop of glue at the knife edges. One average strain measurement was obtained from the two extensometers. In spite of the research team efforts, MTS did not provide a solution to obtain separate strain measurements. The test setup is shown in Figure 3.1.

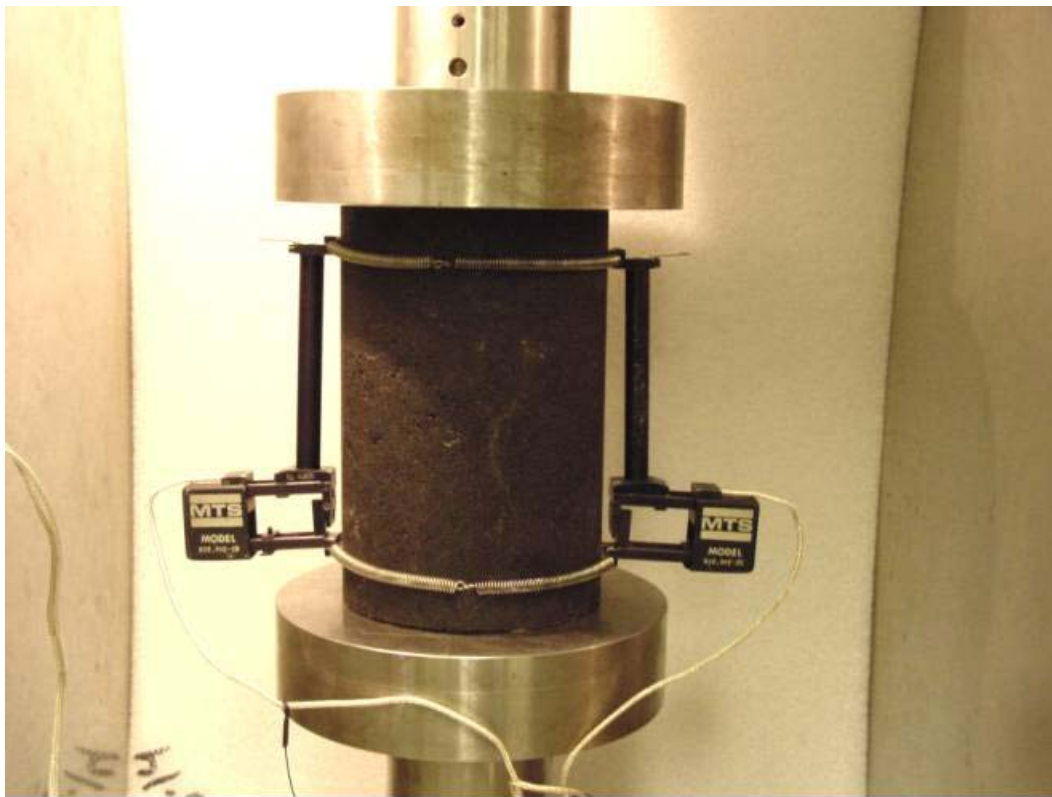


Figure 3.1. Dynamic Modulus Test Setup

All tests were performed inside an environmental chamber (Thermotron Industries Model # FR-3-CH-LN2). Liquid nitrogen tanks were used to cool the chamber below room temperature, and mechanical heating was used for temperatures as high as 54°C. The temperature was controlled by an MTS 409.80 Temperature Controller, and verified by using an independent Omega 869C platinum RTD thermometer.

Sample Preparation

Cylindrical specimens 100-mm by 150-mm were prepared according to NCHRP Project 9-29 [15]. Cylindrical specimens 150-mm by 170-mm specimens were compacted in the laboratory using the Brovold gyratory compactor. They were then cored to a 100-mm diameter and saw cut to a final height of 150 mm. The air voids were measured on the finished test specimens. Adjustments were made to the number of gyrations during compaction to achieve about 5.0% air voids. This sample preparation procedure was done to make four samples for each for three mixtures from Cells 33, 34, and 35, respectively.

For the mixture from Cell 35, an additional four 100-mm by 150-mm samples were prepared using Testquip 100-mm diameter mold that fits inside the 150-mm sleeves for the gyratory compactor. This helped in evaluating if the density gradients incurred during compaction did, in fact, influence the results of dynamic modulus tests. The samples were simply compacted to 100-mm by 150-mm specimens and tested without any further coring or sawing. Significant time and energy could be saved in sample preparation if the results between the two techniques proved indistinguishable.

For the fourth mixture tested, four 150-mm diameter cores were taken from Cell 21 at Mn/ROAD. The same coring and cutting procedures were followed to obtain 100-mm by 150-mm specimens.

Table 3.3 shows the parameters obtained during sample preparation, including air voids, compaction temperature, number of gyrations, height, and diameter of the specimens.

Table 3.3. Sample Preparation Data

| Cell | Sample # | Compaction Temperature, °C | # Gyration | Air Voids | Height, mm | Diameter, mm |
|----------------|-----------|----------------------------|------------|-------------|---------------|---------------|
| 21 | 2102BC005 | -- | -- | 4.5% | 150.33 | 100.33 |
| 21 | 2102BC006 | -- | -- | 3.9% | 160.35 | 100.62 |
| 21 | 2102BC007 | -- | -- | 4.7% | 163.18 | 100.17 |
| 21 | 2102BC008 | -- | -- | 4.3% | 159.86 | 100.60 |
| <i>Average</i> | | | | <i>4.3%</i> | <i>158.43</i> | <i>100.43</i> |
| 33 | 58-28-2 | 133 | 75 | 5.7% | 150.16 | 100.80 |
| 33 | 58-28-3 | 133 | 75 | 5.5% | 157.60 | 100.64 |
| 33 | 58-28-4 | 133 | 75 | 5.9% | 155.02 | 100.61 |
| 33 | 58-28-5 | 133 | 75 | 5.1% | 155.08 | 100.71 |
| <i>Average</i> | | | | <i>5.6%</i> | <i>154.46</i> | <i>100.69</i> |
| 34 | 58-34-1 | 118 | 40 | 4.4% | 149.01 | 100.72 |
| 34 | 58-34-2 | 118 | 40 | 4.1% | 153.74 | 100.47 |
| 34 | 58-34-3 | 118 | 40 | 3.9% | 153.47 | 100.60 |
| 34 | 58-34-4 | 118 | 40 | 4.6% | 148.55 | 100.85 |
| <i>Average</i> | | | | <i>4.3%</i> | <i>151.19</i> | <i>100.66</i> |
| 35 | 58-40-1 | 124 | 40 | 4.8% | 146.98 | 100.58 |
| 35 | 58-40-2 | 124 | 40 | 4.7% | 153.23 | 100.74 |
| 35 | 58-40-3 | 124 | 40 | 4.9% | 154.99 | 100.88 |
| 35 | 58-40-4 | 124 | 40 | 4.8% | 155.05 | 100.61 |
| <i>Average</i> | | | | <i>4.8%</i> | <i>152.56</i> | <i>100.70</i> |
| 35* | 58-40-6 | 124 | 100 | 5.5% | 161.55 | 99.80 |
| 35* | 58-40-7 | 124 | 100 | 6.1% | 162.43 | 99.70 |
| 35* | 58-40-8 | 124 | 100 | 5.2% | 160.84 | 99.81 |
| 35* | 58-40-9 | 124 | 100 | 4.9% | 160.32 | 99.72 |
| <i>Average</i> | | | | <i>5.4%</i> | <i>161.29</i> | <i>99.76</i> |

*NOTE: Samples 58-40-6, 7, 8, and 9 were compacted using slender mold.

Testing Procedures

The testing procedure was based on NCHRP 9-29 proposed standard A1: “Dynamic Modulus of Asphalt Concrete Mixtures and Master Curves” [25]. The recommended procedure involves performing tests at several different temperatures and loading frequencies. Tests were performed at temperatures of -20, -10, 4, 20, 40, and 54°C and frequencies of 25, 10, 1, 0.1, and 0.01 Hz. Each specimen was tested for 29 combinations of temperature and frequency, excluding only 0.01 Hz at 54°C. At very high temperatures and low frequencies, the sample begins to show non-linear effects. Testing began with the lowest temperature and proceeded to the highest. At a given temperature, the testing began with the highest frequency of loading and proceeded to the lowest.

On the night before testing, the extensometers were placed on the test specimen using springs and glue as mentioned above. The specimen was then placed in a freezer overnight at -20°C to ensure temperature equilibrium. On the morning of testing, the specimen was placed in the environmental chamber at -20°C and allowed to equilibrate for 1.5 hours. Teflon paper was placed between the specimen and steel plates at the top and bottom.

To begin testing, the extensometers were zeroed, and a minimal contact load was applied to the specimen. A sinusoidal axial compressive load was applied to the specimen without impact in a cyclic manner. The load was adjusted in each case to attempt to keep the axial strains between 50 and 150 $\mu\epsilon$. The first step was to apply a preconditioning load to the specimen with 200 cycles at 25 Hz. Testing continued with different numbers of cycles for each frequency as shown in Table 3.4. The data acquisition system was set up to record the last six cycles at each frequency with about 200 points per cycle. The task report for the data analysis explains in detail how the raw force and displacement data is manipulated to obtain the dynamic modulus and phase angle for each specimen.

Table 3.4. Cycles for Test Sequence

| Frequency, Hz | Number of Cycles |
|----------------------|-------------------------|
| Preconditioning (25) | 200 |
| 25 | 50 |
| 10 | 50 |
| 1 | 25 |
| 0.1 | 6 |
| 0.01 | 6 |

After the entire cycle of testing was complete at -20°C , the environmental chamber was set to the next temperature. After 1.5 hours conditioning, the above steps were repeated until completion of the entire sequence of temperatures and frequencies.

One difficulty involved keeping the axial strains under 150 $\mu\epsilon$ to ensure test performance in the linear viscoelastic regime. For the most part, the strains were kept under 300 $\mu\epsilon$. However, the cores from Cell 21 had significantly higher strains above 20°C , approaching values as high as 1500 $\mu\epsilon$, although the load levels were adjusted after every test to get the strains to approach the proper range. The test data obtained at these higher strains is most probably nonlinear and should be interpreted correspondingly.

Chapter 4

Results and Discussion

Raw Data

The complex dynamic modulus tests produced large amounts of test data. There were six test temperatures: -20°C , -10°C , 4°C , 20°C , 40°C , and 54°C . For the first five temperatures, there were five frequencies for each temperature: 25 Hz, 10 Hz, 1 Hz, 0.1 Hz, and 0.01 Hz. At 54°C , testing was not performed at a frequency of 0.01 Hz. The tests were performed from the lowest temperature to the highest temperature and from the highest frequency to the lowest frequency.

Data Variables

The test variables obtained from the data acquisition system include the time, axial force, axial displacement, and the displacement from the extensometers. The variable time is the time period from the test start to the data recording time. The axial force is the vertical load on the specimen, and axial displacement is the vertical displacement of the load piston. It is important to note that the displacement for the extensometer is the average value, although two gages were used in the test. Both extensometers had an axial gage length of 114.3 mm. Four specimens were tested for each mixture. Before the tests were performed, the height and diameter for each specimen were measured and the specimen area was calculated. Table 3.3 shows the measured data for these specimen sizes. To arrive at the actual stress under certain test conditions, the axial force was divided by the calculated area of the specimen. Similarly, the extensometer displacement was divided by the axial gage length to arrive at the axial strain for the test under the same test conditions.

For any given test temperature, one data file was acquired for each specimen. The data file starts from 25 Hz and ends at 0.01 Hz for each of the test temperatures except for 54°C , for which ends at 0.1 Hz. At 25 Hz, the test data is obtained from the 45th cycle to the 50th cycle, and there are about 164 data points in each cycle. For 10 Hz, the test data is from the 45th cycle to the 50th cycle, and there are about 204 data points in each cycle. For 1 Hz, the data is from the 20th cycle to the 25th cycle, and there are about 100 data points in each cycle. For 0.1 Hz, the data is

from the first cycle to sixth cycle and about 199 points in each cycle. The data for 0.01 Hz is the same as with the frequency of 0.1 Hz.

In this project, tests were performed for 20 specimens. Four of these specimens are for Cell 21, and the sample numbers are 2102BC005, 2102BC006, 2102BC007, and 2102BC008. Four are for Cell 33, and the sample numbers are 58-28-2, 58-28-3, 58-28-4, and 58-28-5. Four are for Cell 34, and the sample numbers are 58-34-1, 58-34-2, 58-34-3, and 58-34-4. Eight specimens are for Cell 35, and the sample numbers are 58-40-1, 58-40-2, 58-40-3, 58-40-4, 58-40-5, 58-40-6, 58-40-7, and 58-40-8. In the eight specimens for Cell 35, the first four specimens were cored from 150-mm diameter specimens, and the latter four specimens were compacted directly to a 100-mm diameter. The last four specimens here were selected to compare the coring vs. compacting effect to the dynamic modulus and phase angle.

Raw Data Plots

For asphalt concrete, the complex dynamic modulus and phase angle change with the temperature and loading time or loading frequency. At low temperature, the modulus for asphalt concrete is large, so it is easy to control the applied axial force to obtain small displacements. At high temperatures such as 40°C and 54°C, the material becomes soft, and it is very difficult to control the axial force to get small displacements. Figures 4.1 and 4.2 are two typical plots of the raw test data.

Figures 4.1 and 4.2 are typical force and displacement versus time plots at -20°C and 40°C for the frequency 25 Hz. In Figure 4.1, the curves for force and displacement are almost sinusoidal shape. The force curve in Figure 4.2 is sinusoidal as well, while the curve for displacement has a downward drift and the data points are much more scattered than those in Figure 4.1. The possible reasons for this phenomenon can be attributed to (1) the fact that the testing equipment is used close to its resolution limit and (2) material behavior at higher temperatures at which creep and aggregate effects become significant.

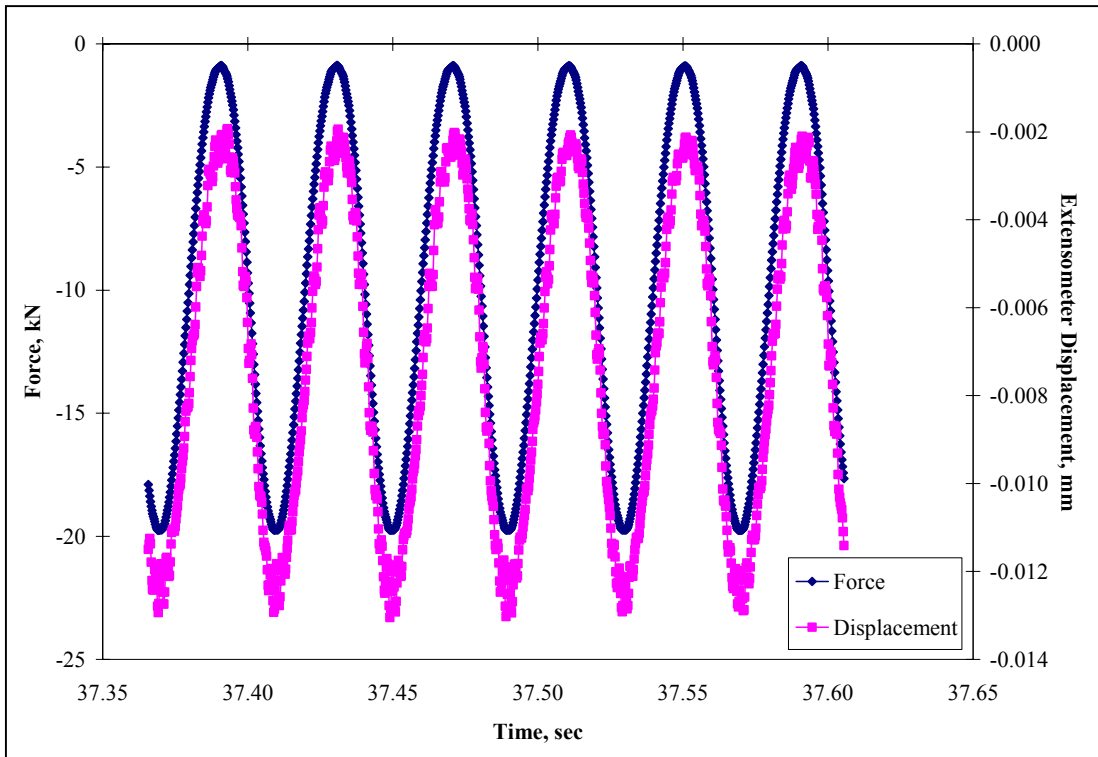


Figure 4.1. Typical Force, Displacement vs. Time Plot at Low Temperature (-20°C)

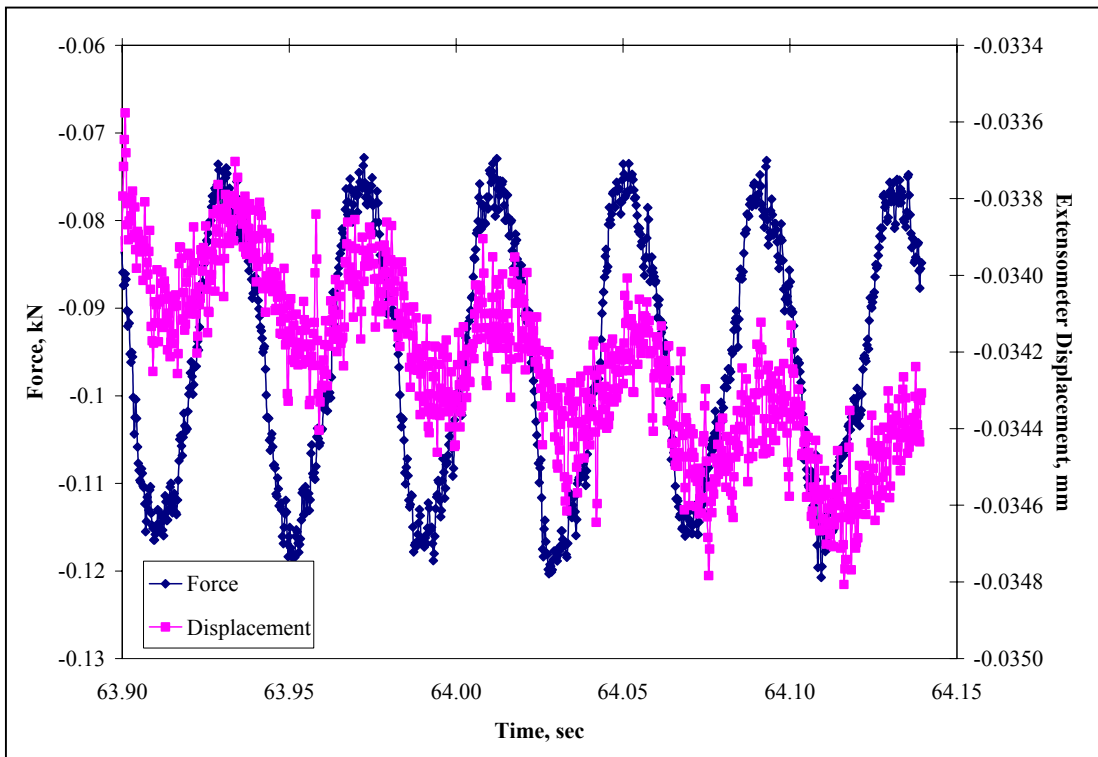


Figure 4.2. Typical Force, Displacement vs. Time Plot at High Temperature (40°C)

Data Analysis Method

The data obtained from the complex modulus test is quite extensive; for one temperature, there are more than 5,000 lines of data for one specimen. To analyze the complex modulus data, this project used a modified version of the SINAAT 2.0 program developed by Don Christensen (Advanced Asphalt Technologies), which is based on the recommendations for the analysis of dynamic data as part of NCHRP 9-29. One modification was to analyze different numbers of data points and different numbers of cycles other than 500 points and 10 cycles. Another modification was to convert the units to SI.

Using the modified program, the test data was copied and pasted from the raw data file into the data worksheet, and the program analyzed the data automatically. The data columns include: Point Number, Time, Vertical Displacement, Vertical Load, two Gage Displacements, and Command Load. Here, the average value from the two extensometers was obtained, so this average value was input to both gage displacement columns. There was no command load data we could acquire from the MTS system, so it was replaced it with the actual axial load. The analysis results included the complex dynamic modulus (GPa), phase angle (degree), and some plots such as normalized load and displacement curves and data traces.

At high temperatures, the displacement curves are not sinusoidal but increase with time, due to the drift in the displacement. The following equations generally represent the load and displacement.

$$F = A_{0F} + C_{1F} * \sin(2\pi f * t + \delta_F) \quad (4.1)$$

$$D = A_{0D} * t + C_{1D} * \sin(2\pi f * t + \delta_D) \quad (4.2)$$

where: F and D = load and displacement respectively;

A_{0F} = mean value for the load;

A_{0D} = slope of the drift curve for the displacement;

C_{1F} and C_{1D} = amplitude specifies the height of the oscillation for the load and displacement respectively;

F = frequency for the test;

δ_F and δ_D = phase angle for the load and displacement respectively.

One can invoke the trigonometric identity for equations (4.1) and (4.2):

$$C_{1F} \sin(2\pi f t + \delta_F) = C_{1F} [\sin(2\pi f t) \cos(\delta_F) + \cos(2\pi f t) \sin(\delta_F)] \quad (4.3)$$

$$F = A_{0F} + C_{1F} * \sin(2\pi f * t + \delta_F) = A_{0F} + A_{1F} \cos(2\pi f t) + B_{1F} \sin(2\pi f t) \quad (4.4)$$

where

$$A_{1F} = C_{1F} \sin(\delta_F) \quad \text{and} \quad B_{1F} = C_{1F} \cos(\delta_F) \quad (4.5)$$

The phase angle and amplitude for the load are obtained as follows [26]:

$$\delta_F = \arctan\left(\frac{A_{1F}}{B_{1F}}\right) \quad (4.6)$$

$$C_{1F} = \sqrt{A_{1F}^2 + B_{1F}^2} \quad (4.7)$$

Using the least-square fit of a sinusoid, the goal is to determine coefficient values that minimize [26]:

$$S_r = \sum_{i=1}^N \{y_i - [A_0 + A_1 \cos(2\pi f t_i) + B_1 \sin(2\pi f t_i)]\}^2 \quad (4.8)$$

The solutions for the equation (4.8) are [26]:

$$A_0 = \frac{\sum Y}{N}, \quad A_1 = \frac{2}{N} \sum Y \cos(2\pi f t) \quad \text{and} \quad B_1 = \frac{2}{N} \sum Y \sin(2\pi f t) \quad (4.9)$$

Here, Y is the centered load from the actual load value, and N is the data point. The four parameters are used to characterize the sinusoidal function for the load.

Maximum and minimum values were obtained every cycle for the displacement. The slope was then calculated for the maximum and minimum value, respectively. The average of these two slopes was interpreted as the drift rate.

Equation (4.9) could be used to calculate the parameters for the displacement. It should be noted that Y should be the corrected displacement. The following equation gives the method for this correction:

$$Y_c = (Y_0 - E) - R * t \quad (4.10)$$

where: Y_c = Corrected displacement;

Y_0 = actual displacement;

E = Average of all the actual displacements;

$(Y_0 - E)$ = centered displacement;

R = displacement drift rate;

t = time.

After the corrected displacement was obtained, equation (4.9) was used to calculate A_0 , A_1 , and B_1 . From these parameters, equations (4.4), (4.5), and (4.6) were used to calculate the amplitude and phase angle for the displacement curve.

Once all the parameters for the load and displacement curve are obtained, it is straightforward to calculate the complex dynamic modulus and phase angle for the asphalt mixture:

$$|E^*| = \frac{C_{1F}}{C_{1D}} * \frac{L_G}{A} \quad (4.11)$$

$$\delta = \delta_F - \delta_D \quad (4.12)$$

where $|E^*|$ and δ = complex modulus and phase angle for the material respectively;

C_{1F} and C_{1D} = amplitude for the load and displacement curve as described above;

L_G = gage length;

A = specimen area;

δ_F and δ_D = phase angle for the load and displacement, respectively.

Analysis of Test Data Results

Test Data

One analysis file was obtained for each load frequency. In this analysis file, the complex dynamic modulus in GPa and the phase angle in degree were obtained for the given test temperature and frequency. There were four replicate specimens tested for each asphalt mixture. After all the complex dynamic modulus and phase angle values were calculated for each specimen under the same test conditions, the average value for both of these parameters was calculated. The standard deviation and coefficient of variation for both dynamic modulus and phase angle also were calculated for each mixture. The following tables contain the average values for the four specimens for each asphalt mixture. Data values that were obvious outliers were discarded.

Table 4.1. Average Dynamic Modulus and Phase Angle for Cell 21

| Temperature, °C | Frequency, Hz | Dynamic Modulus, GPa | Standard Deviation | Coefficient of Variation | Phase Angle, Degree | Standard Deviation | Coefficient of Variation |
|-----------------|---------------|----------------------|--------------------|--------------------------|---------------------|--------------------|--------------------------|
| -20 | 0.01 | 12.0 | 5.95 | 49.8% | 12.2 | 2.69 | 22.0% |
| -20 | 0.1 | 15.1 | 8.79 | 58.4% | 8.5 | 1.80 | 21.1% |
| -20 | 1 | 18.2 | 11.48 | 63.3% | 6.2 | 0.74 | 11.8% |
| -20 | 10 | 19.5 | 12.05 | 62.0% | 6.2 | 0.87 | 14.2% |
| -20 | 25 | 20.6 | 11.85 | 57.5% | 5.4 | 0.92 | 16.9% |
| -10 | 0.01 | 7.3 | 3.76 | 51.5% | 16.1 | 1.35 | 8.4% |
| -10 | 0.1 | 10.4 | 6.15 | 59.0% | 10.9 | 0.78 | 7.2% |
| -10 | 1 | 13.4 | 6.69 | 50.0% | 8.5 | 0.29 | 3.4% |
| -10 | 10 | 16.4 | 6.76 | 41.2% | 6.9 | 1.08 | 15.7% |
| -10 | 25 | 17.4 | 6.20 | 35.6% | 7.6 | 0.74 | 9.7% |
| 4 | 0.01 | 1.7 | 0.10 | 6.1% | 30.7 | 0.87 | 2.8% |
| 4 | 0.1 | 3.2 | 0.33 | 10.4% | 22.7 | 1.89 | 8.3% |
| 4 | 1 | 5.4 | 0.66 | 12.2% | 17.7 | 1.43 | 8.1% |
| 4 | 10 | 9.7 | 4.86 | 50.1% | 12.4 | 1.07 | 8.6% |
| 4 | 25 | 10.6 | 4.80 | 45.1% | 11.6 | 1.19 | 10.2% |
| 20 | 0.01 | 0.3 | 0.05 | 18.2% | 47.8 | 1.68 | 3.5% |
| 20 | 0.1 | 0.7 | 0.17 | 25.3% | 43.6 | 5.70 | 13.1% |
| 20 | 1 | 1.8 | 0.46 | 26.2% | 37.7 | 7.00 | 18.6% |
| 20 | 10 | 3.7 | | | 28.4 | 2.65 | 9.3% |
| 20 | 25 | 4.5 | | | | | |
| 40 | 0.01 | 0.1 | 0.00 | 0.0% | 43.5 | 1.39 | 3.2% |
| 40 | 0.1 | 0.1 | 0.00 | 0.0% | 44.8 | 3.96 | 8.8% |
| 40 | 1 | 0.3 | 0.10 | 40.0% | 38.4 | 3.41 | 8.9% |
| 40 | 10 | | | | | | |
| 40 | 25 | 0.9 | 0.45 | 50.5% | 28.5 | | |
| 54 | 0.01 | | | | | | |
| 54 | 0.1 | 0.1 | 0.00 | 0.0% | 25.1 | 0.58 | 2.3% |
| 54 | 1 | 0.1 | 0.00 | 0.0% | 22.2 | 3.03 | 13.6% |
| 54 | 10 | 0.4 | 0.07 | 20.2% | 36.5 | | |
| 54 | 25 | 0.6 | 0.40 | 66.7% | | | |

Table 4.2. Average Dynamic Modulus and Phase Angle for Cell 33

| Temperature, °C | Frequency, Hz | Dynamic Modulus, GPa | Standard Deviation | Coefficient of Variation | Phase Angle, Degree | Standard Deviation | Coefficient of Variation |
|-----------------|---------------|----------------------|--------------------|--------------------------|---------------------|--------------------|--------------------------|
| -20 | 0.01 | 12.3 | 3.50 | 28.4% | 12.6 | 1.01 | 8.0% |
| -20 | 0.1 | 16.1 | 6.23 | 38.7% | 7.2 | 0.71 | 9.9% |
| -20 | 1 | 19.1 | 6.78 | 35.5% | 6.0 | 0.79 | 13.1% |
| -20 | 10 | 20.5 | 5.89 | 28.7% | 4.6 | 1.62 | 34.9% |
| -20 | 25 | 22.7 | 5.73 | 25.3% | 4.8 | 1.59 | 32.9% |
| -10 | 0.01 | 7.8 | 2.58 | 32.9% | 17.3 | 1.15 | 6.7% |
| -10 | 0.1 | 10.8 | 3.59 | 33.3% | 11.4 | 0.67 | 5.9% |
| -10 | 1 | 13.9 | 4.39 | 31.5% | 8.5 | 1.16 | 13.7% |
| -10 | 10 | 17.1 | 4.84 | 28.4% | 6.8 | 1.23 | 18.1% |
| -10 | 25 | 18.2 | 4.81 | 26.5% | 7.3 | 1.46 | 19.9% |
| 4 | 0.01 | 2.6 | 0.88 | 34.0% | 28.2 | 2.25 | 8.0% |
| 4 | 0.1 | 4.8 | 1.64 | 34.2% | 22.9 | 1.59 | 7.0% |
| 4 | 1 | 7.7 | 2.52 | 32.7% | 16.8 | 0.38 | 2.3% |
| 4 | 10 | 11.1 | 3.24 | 29.3% | 12.2 | 0.57 | 4.7% |
| 4 | 25 | 13.4 | 4.08 | 30.5% | 12.1 | 1.38 | 11.4% |
| 20 | 0.01 | 0.4 | 0.10 | 22.5% | 39.3 | 2.56 | 6.5% |
| 20 | 0.1 | 1.1 | 0.33 | 29.4% | 38.4 | 2.11 | 5.5% |
| 20 | 1 | 2.8 | 0.94 | 34.2% | 32.0 | 2.00 | 6.3% |
| 20 | 10 | | | | 24.1 | 3.04 | 12.6% |
| 20 | 25 | 6.5 | 2.84 | 43.5% | 21.2 | 0.89 | 4.2% |
| 40 | 0.01 | 0.2 | 0.05 | 28.6% | 27.3 | 3.42 | 12.5% |
| 40 | 0.1 | 0.3 | 0.05 | 18.2% | 28.9 | 3.39 | 11.7% |
| 40 | 1 | 0.5 | 0.15 | 28.6% | 32.2 | 3.65 | 11.3% |
| 40 | 10 | 1.3 | 0.33 | 26.5% | 33.9 | 2.93 | 8.7% |
| 40 | 25 | 1.9 | 0.58 | 31.4% | 33.2 | 0.21 | 0.6% |
| 54 | 0.01 | | | | | | |
| 54 | 0.1 | 0.1 | 0.05 | 40.0% | 14.2 | 0.70 | 5.0% |
| 54 | 1 | 0.2 | 0.00 | 0.0% | 18.2 | 1.66 | 9.2% |
| 54 | 10 | 0.3 | 0.12 | 34.6% | 23.7 | 4.03 | 17.0% |
| 54 | 25 | 0.5 | 0.13 | 24.0% | 26.5 | 3.76 | 14.2% |

Table 4.3. Average Dynamic Modulus and Phase Angle for Cell 34

| Temperature, °C | Frequency, Hz | Dynamic Modulus, GPa | Standard Deviation | Coefficient of Variation | Phase Angle, Degree | Standard Deviation | Coefficient of Variation |
|-----------------|---------------|----------------------|--------------------|--------------------------|---------------------|--------------------|--------------------------|
| -20 | 0.01 | 14.2 | 3.02 | 21.3% | 14.9 | 2.30 | 15.5% |
| -20 | 0.1 | 18.4 | 4.70 | 25.6% | 10.0 | 0.88 | 8.8% |
| -20 | 1 | 22.9 | 4.98 | 21.8% | 7.4 | 0.93 | 12.7% |
| -20 | 10 | 26.4 | 5.49 | 20.8% | 5.5 | 1.27 | 23.1% |
| -20 | 25 | 27.2 | 5.36 | 19.7% | 5.8 | 1.22 | 21.1% |
| -10 | 0.01 | 9.4 | 3.59 | 38.3% | 18.8 | 1.56 | 8.3% |
| -10 | 0.1 | 13.8 | 4.97 | 36.1% | 13.0 | 1.57 | 12.1% |
| -10 | 1 | 18.2 | 5.51 | 30.3% | 9.8 | 0.84 | 8.6% |
| -10 | 10 | 21.9 | 4.30 | 19.6% | 7.6 | 1.69 | 22.2% |
| -10 | 25 | 24.1 | 4.59 | 19.0% | 7.1 | 1.60 | 22.5% |
| 4 | 0.01 | 2.5 | 0.62 | 24.5% | 32.1 | 1.30 | 4.1% |
| 4 | 0.1 | 5.0 | 1.39 | 27.8% | 25.2 | 0.34 | 1.3% |
| 4 | 1 | 8.9 | 2.34 | 26.4% | 19.0 | 0.77 | 4.1% |
| 4 | 10 | 12.8 | 2.68 | 20.9% | 14.4 | 1.45 | 10.1% |
| 4 | 25 | 14.9 | 2.78 | 18.6% | 13.3 | 1.57 | 11.8% |
| 20 | 0.01 | 0.4 | 0.08 | 20.4% | 36.6 | 3.67 | 10.0% |
| 20 | 0.1 | 1.0 | 0.25 | 25.6% | 38.3 | 1.62 | 4.2% |
| 20 | 1 | 2.4 | 0.56 | 23.3% | 33.0 | 3.93 | 11.9% |
| 20 | 10 | 5.6 | 1.06 | 19.1% | 24.2 | 6.80 | 28.0% |
| 20 | 25 | 7.0 | 1.00 | 14.4% | 20.7 | 1.65 | 8.0% |
| 40 | 0.01 | 0.1 | 0.05 | 40.0% | 27.0 | 3.83 | 14.2% |
| 40 | 0.1 | 0.2 | 0.00 | 0.0% | 25.4 | 3.29 | 13.0% |
| 40 | 1 | 0.4 | 0.06 | 16.5% | 27.0 | 4.54 | 16.8% |
| 40 | 10 | | | | | | |
| 40 | 25 | 1.0 | 0.39 | 38.5% | 29.6 | | |
| 54 | 0.01 | | | | | | |
| 54 | 0.1 | 0.2 | 0.06 | 38.5% | 16.7 | 2.57 | 15.4% |
| 54 | 1 | 0.2 | 0.00 | 0.0% | 17.0 | 2.86 | 16.9% |
| 54 | 10 | 0.4 | 0.12 | 31.5% | 25.9 | 5.37 | 20.7% |
| 54 | 25 | 0.5 | 0.08 | 16.3% | 28.1 | 7.19 | 25.6% |

Table 4.4. Average Dynamic Modulus and Phase Angle for Cell 35 (Cored)

| Temperature, °C | Frequency, Hz | Dynamic Modulus, GPa | Standard Deviation | Coefficient of Variation | Phase Angle, Degree | Standard Deviation | Coefficient of Variation |
|-----------------|---------------|----------------------|--------------------|--------------------------|---------------------|--------------------|--------------------------|
| -20 | 0.01 | 7.0 | 1.00 | 14.4% | 16.9 | 1.09 | 6.5% |
| -20 | 0.1 | 9.3 | 1.21 | 13.1% | 13.2 | 1.96 | 14.9% |
| -20 | 1 | 12.0 | 1.28 | 10.7% | 9.9 | 0.79 | 8.0% |
| -20 | 10 | 14.8 | 1.42 | 9.6% | 8.1 | 1.01 | 12.5% |
| -20 | 25 | 16.0 | 1.78 | 11.1% | 7.3 | 0.87 | 11.9% |
| -10 | 0.01 | 3.1 | 0.92 | 29.4% | 20.7 | 0.88 | 4.3% |
| -10 | 0.1 | 4.7 | 1.12 | 23.7% | 15.7 | 0.64 | 4.1% |
| -10 | 1 | 7.9 | 0.80 | 10.1% | 13.4 | 0.40 | 3.0% |
| -10 | 10 | 12.0 | 1.77 | 14.7% | 10.3 | 0.79 | 7.6% |
| -10 | 25 | 13.2 | 2.29 | 17.3% | 9.8 | 0.42 | 4.2% |
| 4 | 0.01 | 1.0 | 0.30 | 31.6% | 28.1 | 2.04 | 7.3% |
| 4 | 0.1 | 1.8 | 0.66 | 36.9% | 25.2 | 1.10 | 4.4% |
| 4 | 1 | 3.1 | 1.07 | 34.6% | 20.5 | 0.83 | 4.0% |
| 4 | 10 | 5.2 | 1.90 | 36.8% | 15.1 | 0.65 | 4.3% |
| 4 | 25 | 6.5 | 1.13 | 17.3% | 15.2 | 0.45 | 3.0% |
| 20 | 0.01 | 0.2 | 0.05 | 22.2% | 32.3 | 2.81 | 8.7% |
| 20 | 0.1 | 0.4 | 0.15 | 35.3% | 31.7 | 2.66 | 8.4% |
| 20 | 1 | 0.9 | 0.46 | 50.2% | 27.7 | 3.83 | 13.8% |
| 20 | 10 | 1.7 | 0.99 | 58.2% | 23.3 | | |
| 20 | 25 | 2.0 | 1.19 | 60.1% | 20.5 | 0.07 | 0.3% |
| 40 | 0.01 | 0.1 | 0.00 | 0.0% | 25.5 | 2.19 | 8.6% |
| 40 | 0.1 | 0.1 | 0.00 | 0.0% | 25.5 | 4.33 | 17.0% |
| 40 | 1 | 0.2 | 0.05 | 22.2% | 23.7 | 1.45 | 6.1% |
| 40 | 10 | 0.4 | 0.05 | 13.3% | 23.4 | 0.14 | 0.6% |
| 40 | 25 | 0.6 | 0.21 | 35.9% | | | |
| 54 | 0.01 | | | | | | |
| 54 | 0.1 | 0.1 | 0.00 | 0.0% | 20.1 | 2.89 | 14.4% |
| 54 | 1 | 0.2 | 0.05 | 28.6% | 17.1 | 2.17 | 12.7% |
| 54 | 10 | 0.3 | 0.08 | 27.2% | | | |
| 54 | 25 | 0.4 | 0.25 | 58.1% | 13.6 | | |

Table 4.5. Average Dynamic Modulus and Phase Angle for Cell 35 (Compacted)

| Temperature, °C | Frequency, Hz | Dynamic Modulus, GPa | Standard Deviation | Coefficient of Variation | Phase Angle, Degree | Standard Deviation | Coefficient of Variation |
|-----------------|---------------|----------------------|--------------------|--------------------------|---------------------|--------------------|--------------------------|
| -20 | 0.01 | 11.0 | 1.86 | 16.9% | 14.4 | 2.21 | 15.3% |
| -20 | 0.1 | 15.0 | 1.94 | 13.0% | 10.6 | 1.70 | 16.1% |
| -20 | 1 | 19.0 | 1.92 | 10.1% | 8.2 | 0.79 | 9.7% |
| -20 | 10 | 22.8 | 1.76 | 7.7% | 7.6 | 1.56 | 20.5% |
| -20 | 25 | 24.3 | 1.63 | 6.7% | 6.3 | 0.74 | 11.8% |
| -10 | 0.01 | 6.3 | 0.68 | 10.8% | 21.2 | 0.92 | 4.3% |
| -10 | 0.1 | 9.5 | 0.83 | 8.7% | 15.4 | 1.14 | 7.4% |
| -10 | 1 | 13.3 | 0.95 | 7.2% | 12.3 | 0.59 | 4.8% |
| -10 | 10 | 17.5 | 1.00 | 5.7% | 9.9 | 0.52 | 5.3% |
| -10 | 25 | 19.1 | 1.02 | 5.4% | 9.2 | 0.52 | 5.7% |
| 4 | 0.01 | 1.8 | 0.19 | 10.4% | 26.6 | 0.33 | 1.2% |
| 4 | 0.1 | 3.3 | 0.36 | 10.8% | 25.2 | 0.59 | 2.3% |
| 4 | 1 | 5.8 | 0.53 | 9.1% | 21.3 | 0.54 | 2.5% |
| 4 | 10 | 9.5 | 0.31 | 3.3% | 17.1 | 0.99 | 5.8% |
| 4 | 25 | 10.6 | 0.74 | 7.0% | 16.0 | 0.56 | 3.5% |
| 20 | 0.01 | 0.4 | 0.13 | 33.6% | 28.7 | 1.50 | 5.2% |
| 20 | 0.1 | 0.7 | 0.24 | 35.0% | 34.4 | 4.67 | 13.6% |
| 20 | 1 | 1.4 | 0.42 | 31.1% | 29.2 | 2.35 | 8.0% |
| 20 | 10 | | | | | | |
| 20 | 25 | 3.6 | 2.28 | 64.1% | 12.3 | | |
| 40 | 0.01 | 0.1 | 0.05 | 40.0% | 27.7 | 4.91 | 17.8% |
| 40 | 0.1 | 0.2 | 0.05 | 28.6% | 26.5 | 4.91 | 18.5% |
| 40 | 1 | 0.4 | 0.10 | 25.5% | 25.5 | 2.37 | 9.3% |
| 40 | 10 | 0.8 | 0.21 | 28.3% | | | |
| 40 | 25 | 0.9 | 0.35 | 40.5% | 18.2 | | |
| 54 | 0.01 | | | | | | |
| 54 | 0.1 | 0.2 | 0.06 | 38.5% | 21.2 | 3.43 | 16.2% |
| 54 | 1 | 0.2 | 0.00 | 0.0% | 18.2 | 1.30 | 7.1% |
| 54 | 10 | 0.5 | 0.23 | 43.3% | | | |
| 54 | 25 | 0.7 | 0.36 | 50.8% | 11.3 | | |

From the above tables, it was observed that the dynamic modulus values for Cell 21 have rather high coefficient of variation values, approaching 50 to 70 percent. These specimens have been cored from a pavement built nine years ago that was subject to traffic and environmental loads during that time. In general, the other cells had much lower coefficient of variation (COV) values, in the range of 20 to 40 percent. The compacted specimens from Cell 35 had the smallest COV values, often under 10 percent. It is possible that coring introduces defects in the specimen that increase the variability of the test measurements. The COV for phase angle for all cells was considerably lower than that of modulus. It generally ranged from 5 to 15 percent at low frequencies to as high as 20 percent as the frequency increased to 10 Hz and 25 Hz.

Figures 4.3 to 4.12 show the average dynamic modulus and phase angle plotted versus frequency for all the asphalt mixtures.

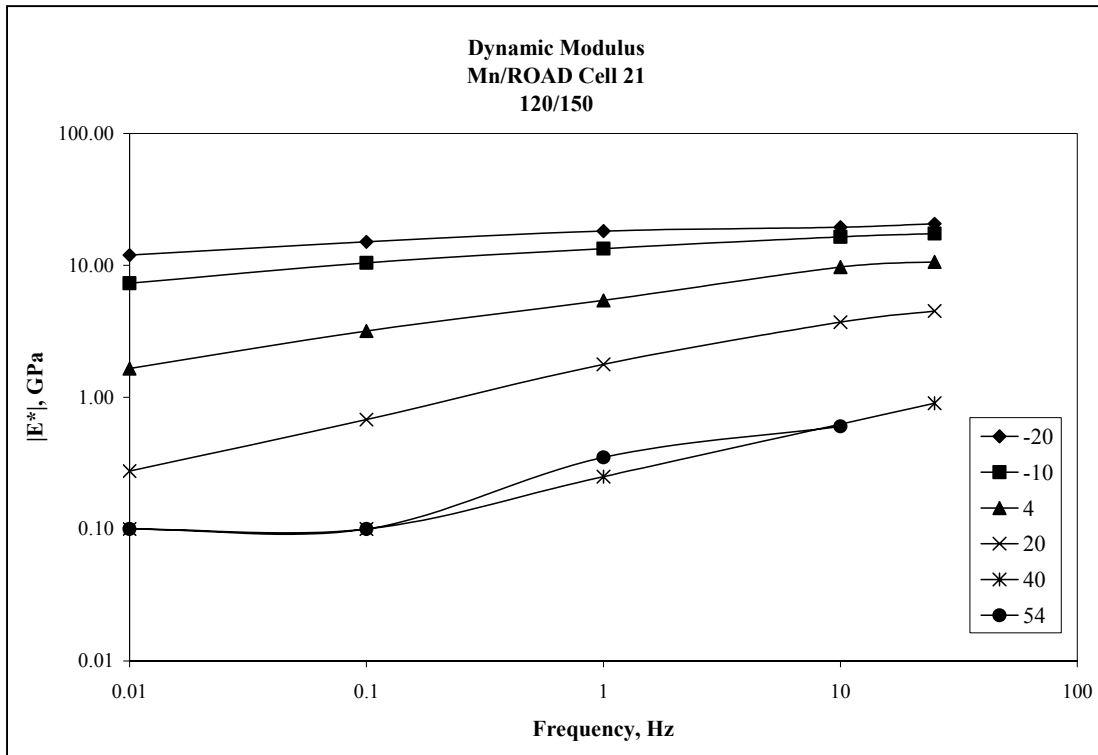


Figure 4.3. Dynamic Modulus vs. Frequency for Cell 21

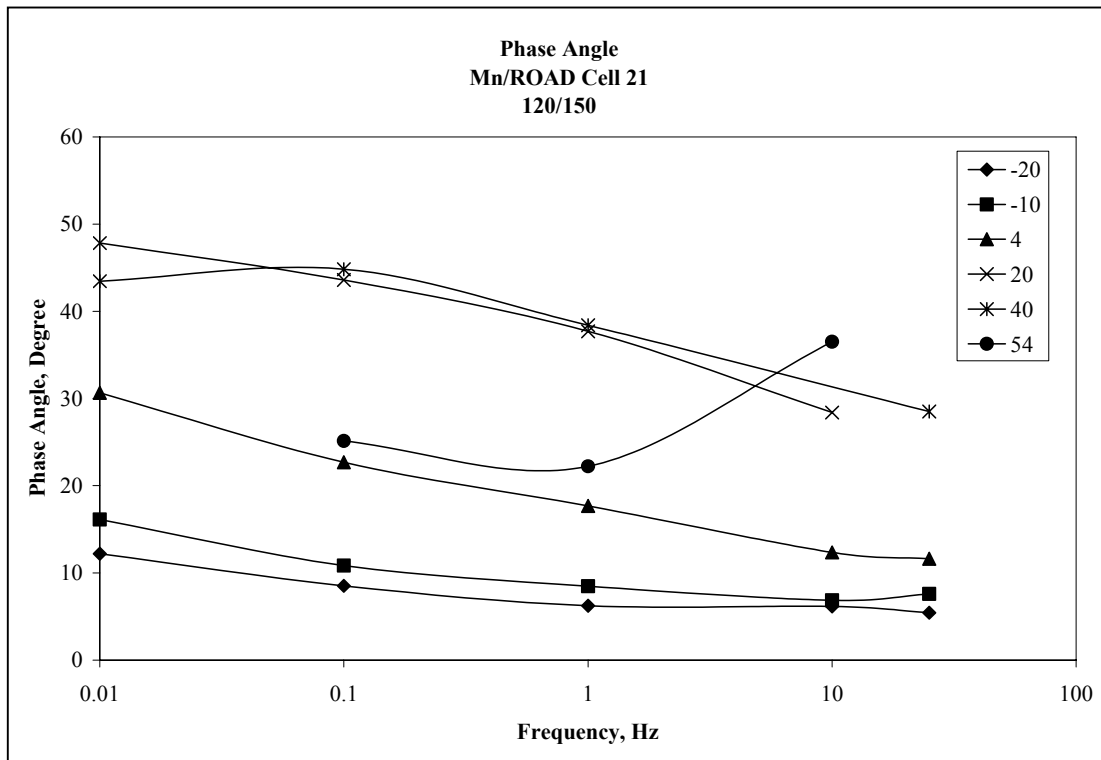


Figure 4.4. Phase Angle vs. Frequency for Cell 21

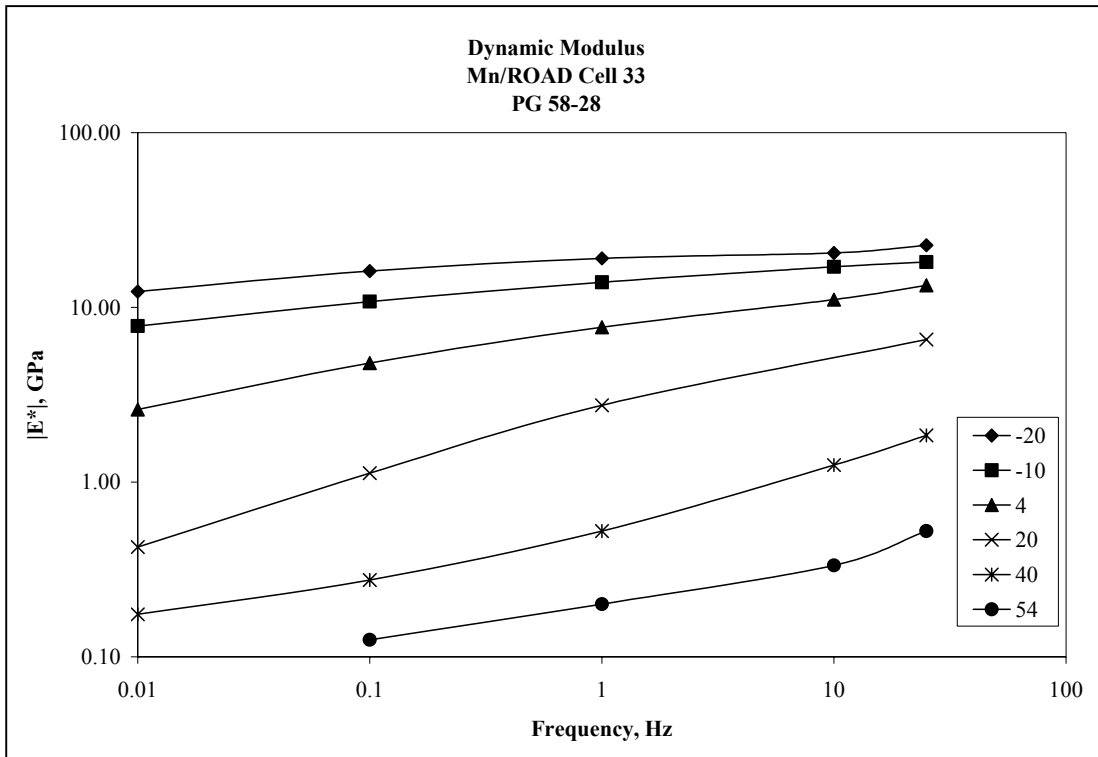


Figure 4.5. Dynamic Modulus vs. Frequency for Cell 33

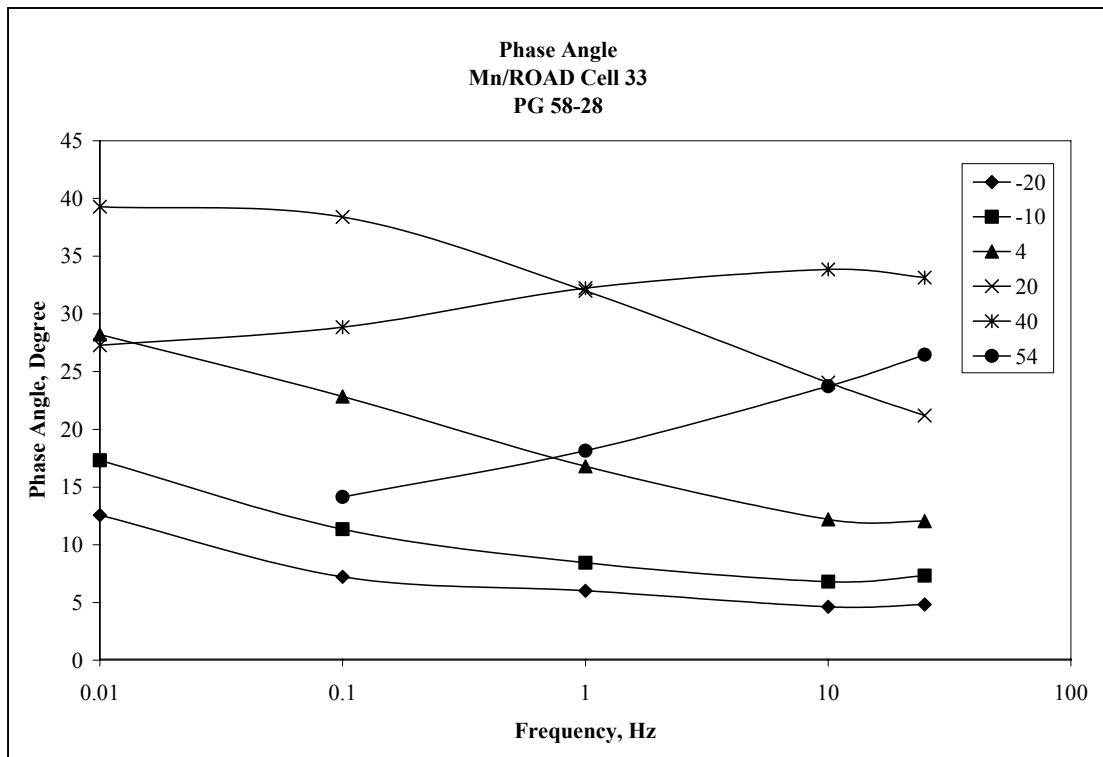


Figure 4.6. Phase Angle vs. Frequency for Cell 33

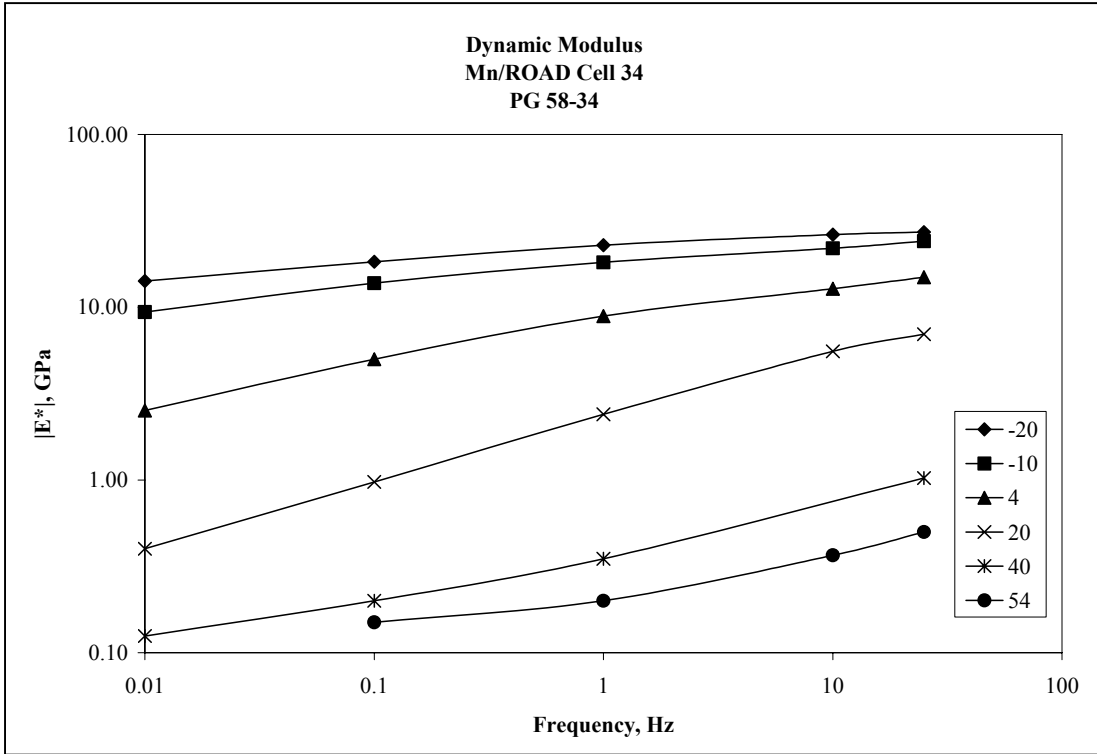


Figure 4.7. Dynamic Modulus vs. Frequency for Cell 34

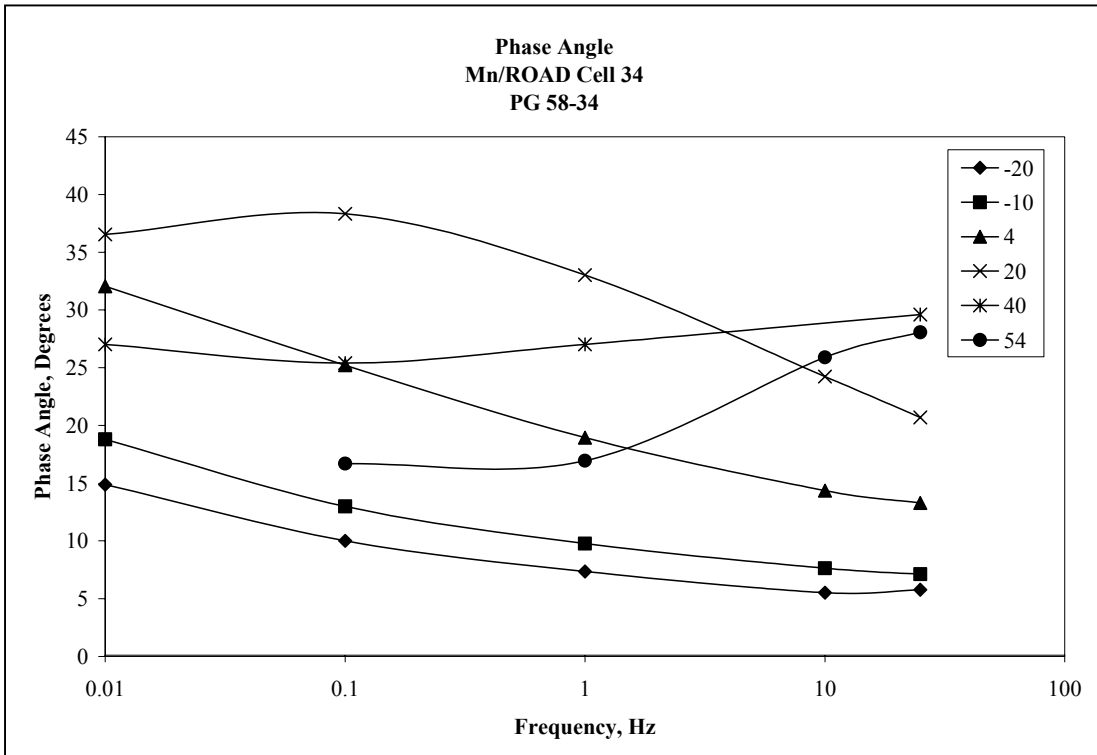


Figure 4.8. Phase Angle vs. Frequency for Cell 34

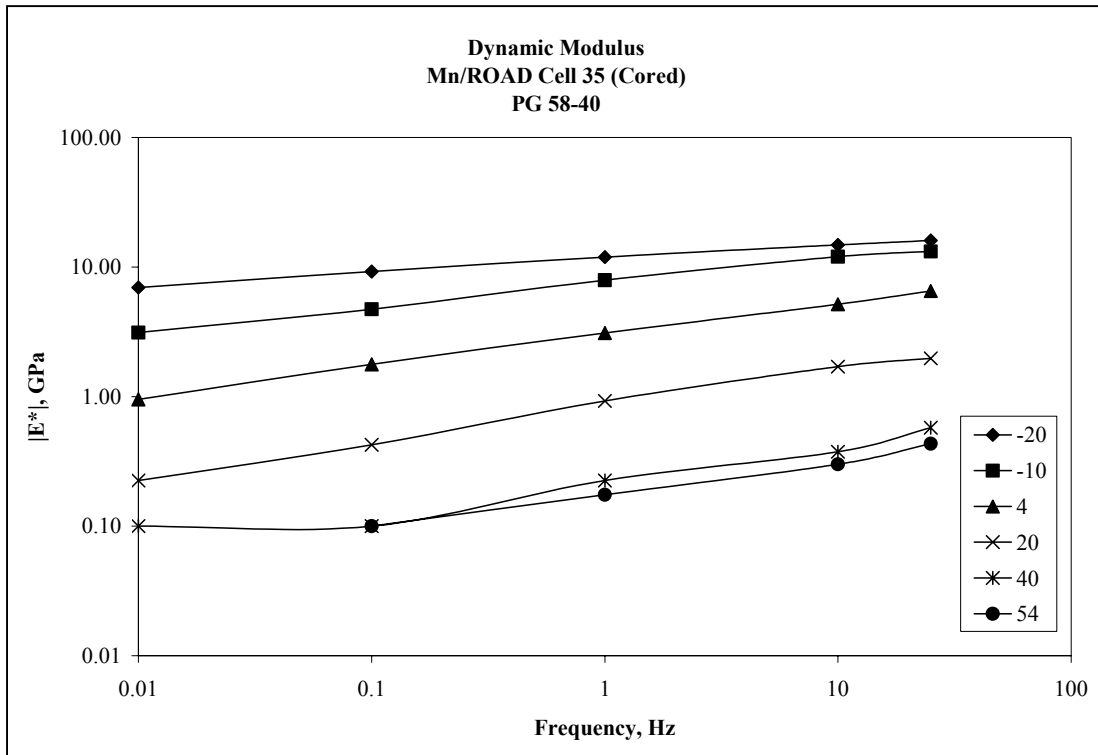


Figure 4.9. Dynamic Modulus vs. Frequency for Cell 35 (Cored)

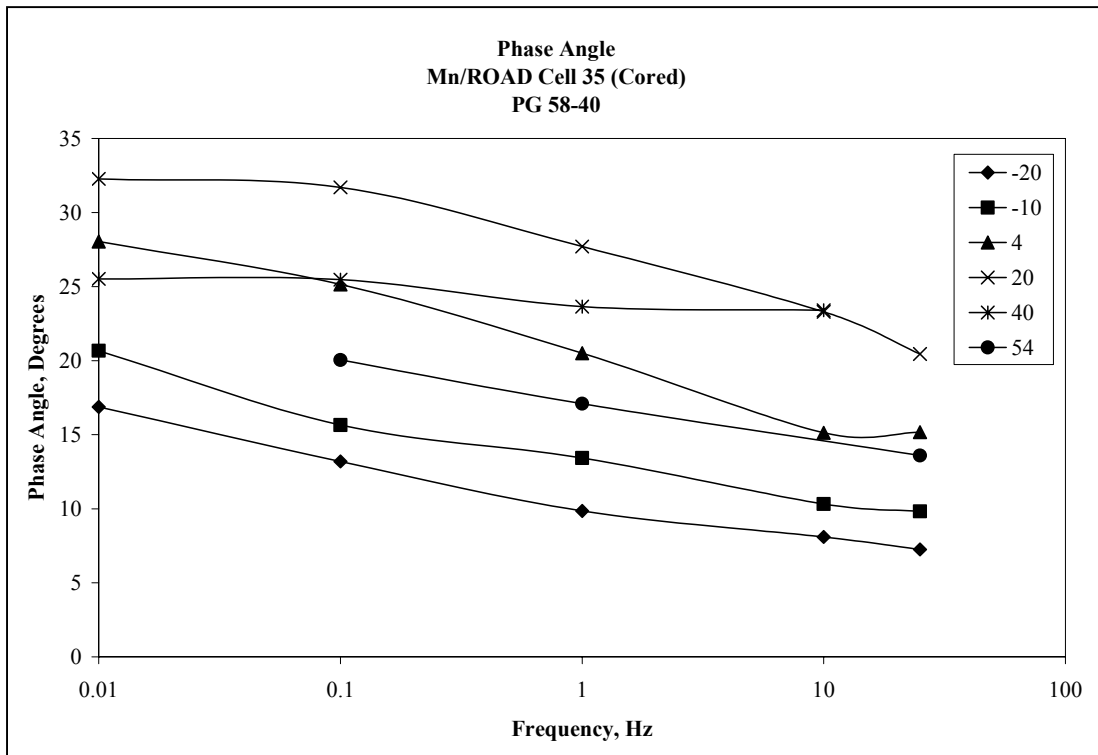


Figure 4.10. Phase Angle vs. Frequency for Cell 35 (Cored)

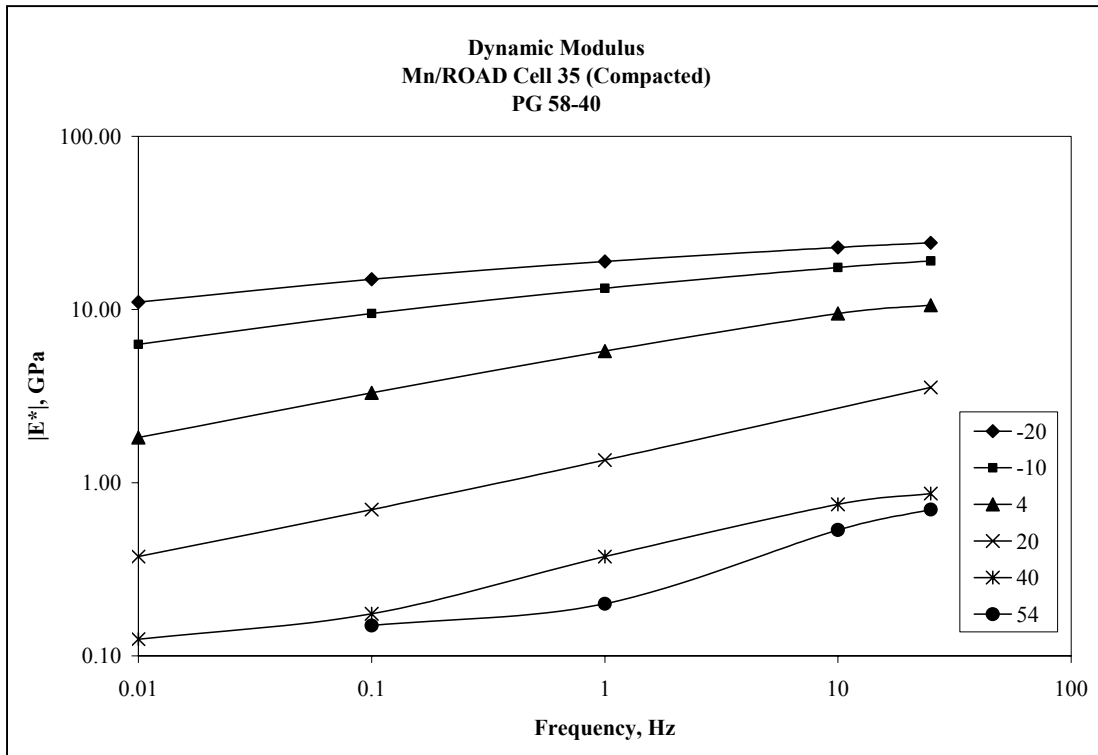


Figure 4.11. Dynamic Modulus vs. Frequency for Cell 35 (Compacted)

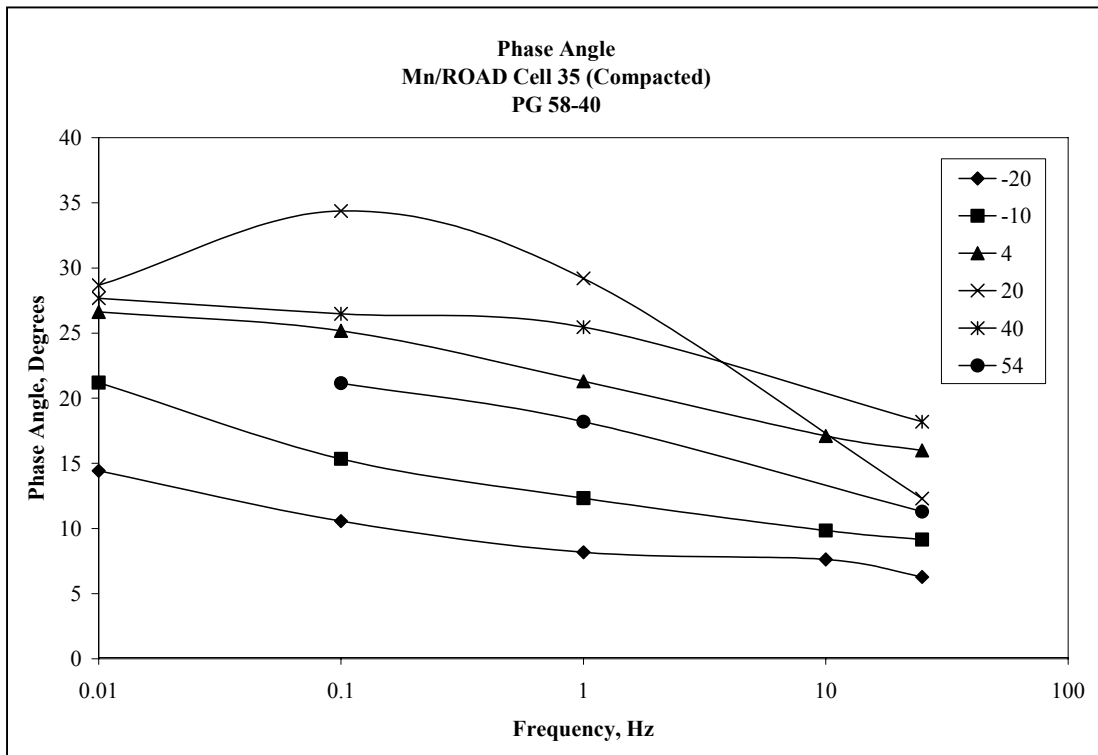


Figure 4.12. Phase Angle vs. Frequency for Cell 35 (Compacted)

The above plots of dynamic modulus and phase angle show the following trends:

1. Under a constant loading frequency, the dynamic modulus decreases with the increase of the test temperature for the same mixture.
2. The phase angle increases with the increase of test temperature from -20°C to 20°C, but for 40°C and 54°C the phase angle decreases with the increase of the test temperature, an indication of aggregate interlock effects.
3. Under a constant test temperature, the dynamic modulus increases with the increase of the test frequency, while most of the phase angle data shows the opposite trend.
4. The dynamic modulus data shows relatively smooth trends, while the phase angle data (especially the data obtained at high test temperatures) shows much more scatter. This means that it is very difficult to obtain accurate test data for phase angle, especially at high test temperatures.

The above trends are consistent with the research results reported by others.

Comparison of Cell 35 Mixtures

In this project, there are two groups of specimens for Cell 35: the first one consists of specimens cored from 150-mm diameter specimens; the second one consists of specimens compacted directly to 100 mm in diameter. The purpose of this study in sample preparation was to evaluate the effect of coring vs. compacting on the properties of the mixture through the comparison of the test results. The test results are shown in Figures 4.13 and 4.14.

It was observed that under the same test conditions, the dynamic modulus for the cored specimens was smaller than the dynamic modulus for the compacted specimens by approximately 40 to 50 percent, while the phase angle results for the cored group were larger than the phase angle for the compacted group by approximately 10 to 20 percent except for a few selected test points. The volumetric data measured before the tests indicates that the average air voids for the cored and compacted group specimens are 4.8 percent and 5.4 percent, respectively. This means that the compacted group has 0.6 percent greater air voids than the cored group and also has the greater dynamic modulus. While there is not a definite answer as to why the specimens exhibit this behavior, a number of factors may apply. These include:

- The cored group have an average height-to-diameter ratio of 1.51, while the compacted group has a h/d ratio of 1.62.

- The air voids for each group were taken from an average of four specimens. Some of the values overlapped. Furthermore, 0.6 percent difference in air voids may not be significant.
- The two groups of samples were taken from different buckets at different locations along the pavement. While they were both from the same mix design, slight changes in asphalt content, gradation, etc. could cause differences in dynamic modulus values.
- The cored specimens likely had rather uniform air voids throughout the specimen. The compacted specimens probably contained density gradients axially and radially throughout the specimens.

The dynamic modulus and phase angle data were further used, as described in the next section, to construct master curves for all the asphalt mixtures at a reference temperature of 20°C.

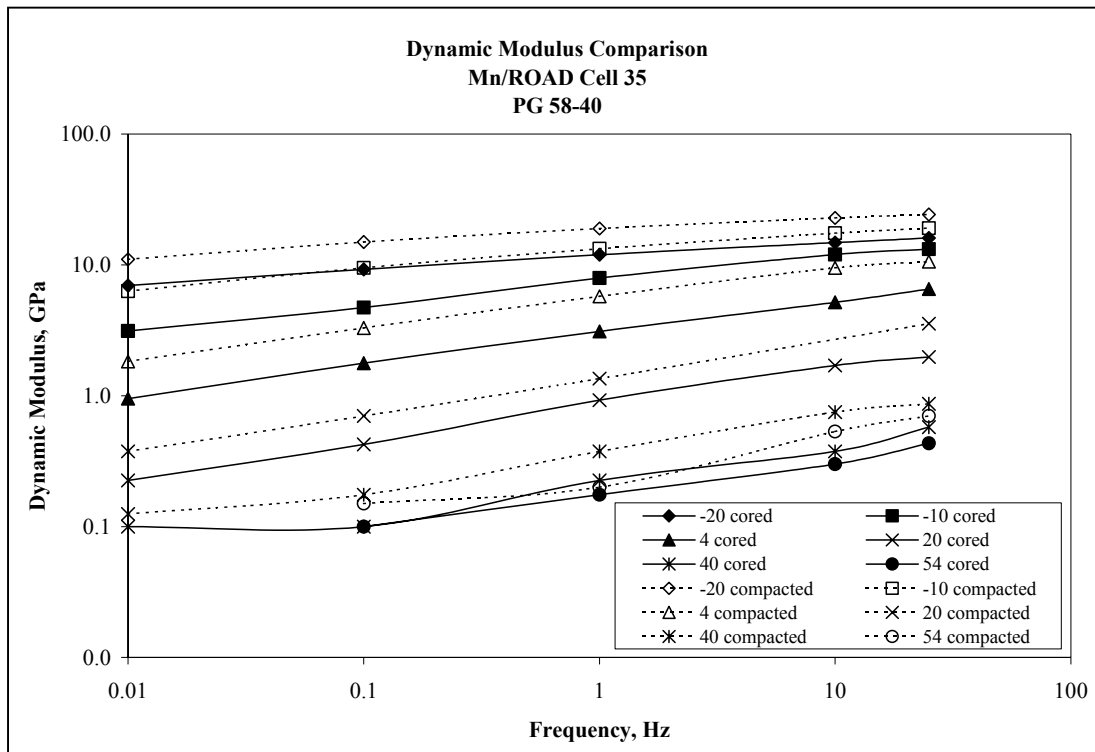


Figure 4.13. Dynamic Modulus Comparison for Cell 35

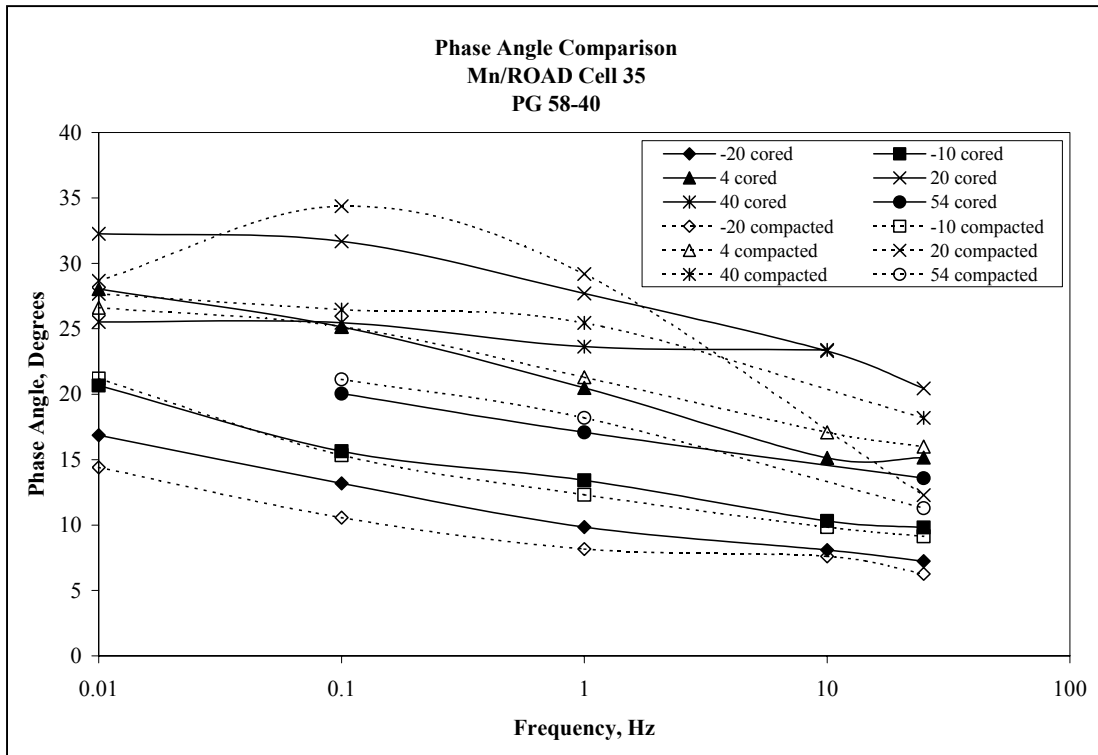


Figure 4.14. Phase Angle Comparison for Cell 35

Master Curves

As previously described, the dynamic modulus and phase angle of asphalt mixtures can be shifted along the frequency axis to form single characteristic master curves at a desired reference temperature or frequency. This procedure assumes that asphalt mixtures are thermorheologically simple materials and that the time-temperature superposition principle is applicable.

Typically the shift factors α_T are obtained from the WLF equation [14]:

$$\log \alpha_T = \frac{C_1(T - T_s)}{C_2 + T - T_s} \quad (4.13)$$

where C_1 and C_2 are constants, T_s is the reference temperature, and T is the temperature of each individual test.

A new method of developing the master curve for asphalt mixtures was developed in the research conducted by Pellinen [16] at the University of Maryland. In this study, master curves were constructed fitting a sigmoidal function to the measured compressive dynamic modulus test data using non-linear least squares regression techniques [16]. The shift can be done by solving

the shift factors simultaneously with the coefficients of the sigmoidal function. The sigmoidal function is defined by equation (4.14). This equation is similar to equation (2.11) in the literature review [15], with the addition of the shift factor in the exponential term as the only change.

$$\log|E^*| = \delta + \frac{\alpha}{1 + e^{\beta - \gamma(\log(f_r) + s_T)}} \quad (4.14)$$

where

$\log|E^*|$ = log of dynamic modulus,

δ = minimum modulus value,

f_r = reduced frequency,

α = span of modulus values,

s_T = shift factor according to temperature, and

β, γ = shape parameters.

The master curve can be constructed using any non-linear curve-fitting technique.

Master Curves from the Test Data

The method above was used to construct master curves using the data in Tables 4.1 to 4.5. The reference temperature for all mixture was 20°C. The commercial computer program SigmaStat was used to fit the master curve for each set of data. This program uses the Marquardt-Levenberg algorithm to find the parameters that give the "best fit" between the equation and the data. The nonlinear regression algorithm seeks the values of the parameters that minimize the sum of the squared differences between the values of the observed and predicted values of the dynamic modulus. Table 4.6 shows the data calculated from the model (equation 4.14) using SigmaStat based on the experimental data. Table 4.7 shows the fitted model parameters for each mixture.

Table 4.6. Dynamic Modulus Data Fit to Model

| Temperature °C | Frequency Hz | Cell 21 | | Cell 33 | | Cell 34 | | Cell 35 (cored) | | Cell 35 (compact) | |
|-------------------|-----------------|------------|---------------------------|------------|---------------------------|------------|---------------------------|-----------------|---------------------------|-------------------|---------------------------|
| | | E* GPa | E* _{fit} GPa | E* GPa | E* _{fit} GPa | E* GPa | E* _{fit} GPa | E* GPa | E* _{fit} GPa | E* GPa | E* _{fit} GPa |
| -20 | 0.01 | 12.0 | 12.3 | 12.3 | 12.8 | 14.2 | 14.4 | 7.0 | 6.6 | 11.0 | 11.0 |
| -20 | 0.1 | 15.1 | 15.2 | 16.1 | 16.0 | 18.4 | 18.9 | 9.3 | 9.5 | 15.0 | 15.1 |
| -20 | 1 | 18.2 | 17.3 | 19.1 | 18.4 | 22.9 | 22.4 | 12.0 | 12.5 | 19.0 | 19.1 |
| -20 | 10 | 19.5 | 18.7 | 20.5 | 20.0 | 26.4 | 24.8 | 14.8 | 15.2 | 22.8 | 22.6 |
| -20 | 25 | 20.6 | 19.0 | 22.7 | 20.4 | 27.2 | 25.4 | 16.0 | 16.2 | 24.3 | 23.9 |
| -10 | 0.01 | 7.3 | 7.1 | 7.8 | 7.4 | 9.4 | 9.1 | 3.1 | 3.1 | 6.3 | 6.2 |
| -10 | 0.1 | 10.4 | 10.7 | 10.8 | 11.2 | 13.8 | 14.1 | 4.7 | 5.2 | 9.5 | 9.6 |
| -10 | 1 | 13.4 | 14.0 | 13.9 | 14.7 | 18.2 | 18.7 | 7.9 | 8.0 | 13.3 | 13.5 |
| -10 | 10 | 16.4 | 16.4 | 17.1 | 17.5 | 21.9 | 22.3 | 12.0 | 11.0 | 17.5 | 17.6 |
| -10 | 25 | 17.4 | 17.2 | 18.2 | 18.3 | 24.1 | 23.4 | 13.2 | 12.2 | 19.1 | 19.1 |
| 4 | 0.01 | 1.7 | 1.4 | 2.6 | 2.4 | 2.5 | 2.3 | 1.0 | 0.9 | 1.8 | 1.8 |
| 4 | 0.1 | 3.2 | 3.3 | 4.8 | 4.8 | 5.0 | 5.0 | 1.8 | 1.8 | 3.3 | 3.4 |
| 4 | 1 | 5.4 | 6.2 | 7.7 | 8.3 | 8.9 | 9.3 | 3.1 | 3.2 | 5.8 | 5.8 |
| 4 | 10 | 9.7 | 9.8 | 11.1 | 12.1 | 12.8 | 14.3 | 5.2 | 5.4 | 9.5 | 9.2 |
| 4 | 25 | 10.6 | 11.3 | 13.4 | 13.5 | 14.9 | 16.2 | 6.5 | 6.5 | 10.6 | 10.7 |
| 20 | 0.01 | 0.3 | 0.3 | 0.4 | 0.5 | 0.4 | 0.4 | 0.2 | 0.2 | 0.4 | 0.4 |
| 20 | 0.1 | 0.7 | 0.7 | 1.1 | 1.1 | 1.0 | 1.0 | 0.4 | 0.4 | 0.7 | 0.7 |
| 20 | 1 | 1.8 | 1.7 | 2.8 | 2.4 | 2.4 | 2.3 | 0.9 | 0.8 | 1.4 | 1.4 |
| 20 | 10 | 3.7 | 3.7 | | | 5.6 | 5.1 | 1.7 | 1.7 | | |
| 20 | 25 | 4.5 | 4.8 | 6.5 | 6.2 | 7.0 | 6.7 | 2.0 | 2.1 | 3.6 | 3.4 |
| 40 | 0.01 | 0.1 | 0.1 | 0.2 | 0.2 | 0.1 | 0.1 | 0.1 | 0.1 | 0.1 | 0.1 |
| 40 | 0.1 | 0.1 | 0.1 | 0.3 | 0.3 | 0.2 | 0.2 | 0.1 | 0.1 | 0.2 | 0.2 |
| 40 | 1 | 0.3 | 0.3 | 0.5 | 0.6 | 0.4 | 0.3 | 0.2 | 0.2 | 0.4 | 0.4 |
| 40 | 10 | | | 1.3 | 1.3 | | | 0.4 | 0.4 | 0.8 | 0.7 |
| 40 | 25 | 0.9 | 0.8 | 1.9 | 1.8 | 1.0 | 1.0 | 0.6 | 0.5 | 0.9 | 0.9 |
| 54 | 0.1 | 0.1 | 0.1 | 0.1 | 0.1 | 0.2 | 0.1 | 0.1 | 0.1 | 0.2 | 0.1 |
| 54 | 1 | 0.1 | 0.2 | 0.2 | 0.2 | 0.2 | 0.2 | 0.2 | 0.2 | 0.2 | 0.3 |
| 54 | 10 | 0.4 | 0.3 | 0.3 | 0.4 | 0.4 | 0.4 | 0.3 | 0.3 | 0.5 | 0.5 |
| 54 | 25 | 0.6 | 0.5 | 0.5 | 0.5 | 0.5 | 0.5 | 0.4 | 0.4 | 0.7 | 0.6 |

Table 4.7. Model Fit Parameters

| Parameter | Cell 21 | Cell 33 | Cell 34 | Cell 35 (cored) | Cell 35 (compact) |
|----------------------------|---------|---------|---------|-----------------|-------------------|
| <i>alpha</i> | 2.8001 | 2.5871 | 2.5949 | 2.9418 | 3.1978 |
| <i>delta</i> | -1.4848 | -1.2369 | -1.1440 | -1.5683 | -1.6656 |
| <i>beta</i> | -0.4401 | -0.5222 | -0.3381 | -0.0353 | -0.2603 |
| <i>gamma</i> | -0.5628 | -0.5515 | -0.5771 | -0.4037 | -0.3734 |
| <i>s_T</i> (-20) | 5.5562 | 5.1745 | 4.9847 | 5.5165 | 5.8844 |
| <i>s_T</i> (-10) | 4.0800 | 3.7277 | 3.9352 | 4.0097 | 4.5037 |
| <i>s_T</i> (4) | 1.8408 | 1.9699 | 1.9663 | 2.0868 | 2.3957 |
| <i>s_T</i> (20) | 0 | 0 | 0 | 0 | 0 |
| <i>s_T</i> (40) | -2.1487 | -1.8129 | -2.3905 | -2.1069 | -1.9814 |
| <i>s_T</i> (54) | -2.7979 | -3.4061 | -3.2517 | -2.4968 | -2.5305 |

Once the shift factors for each test temperature were obtained, the master curve for each asphalt mixture was built. Figure 4.15 shows the master curves fit from equation (4.14) for the five mixtures. Figures 4.16 to 4.20 show the master curves for each individual mixture along with the actual test data. Figure 4.21 plots the shift factor against temperature for each mixture.

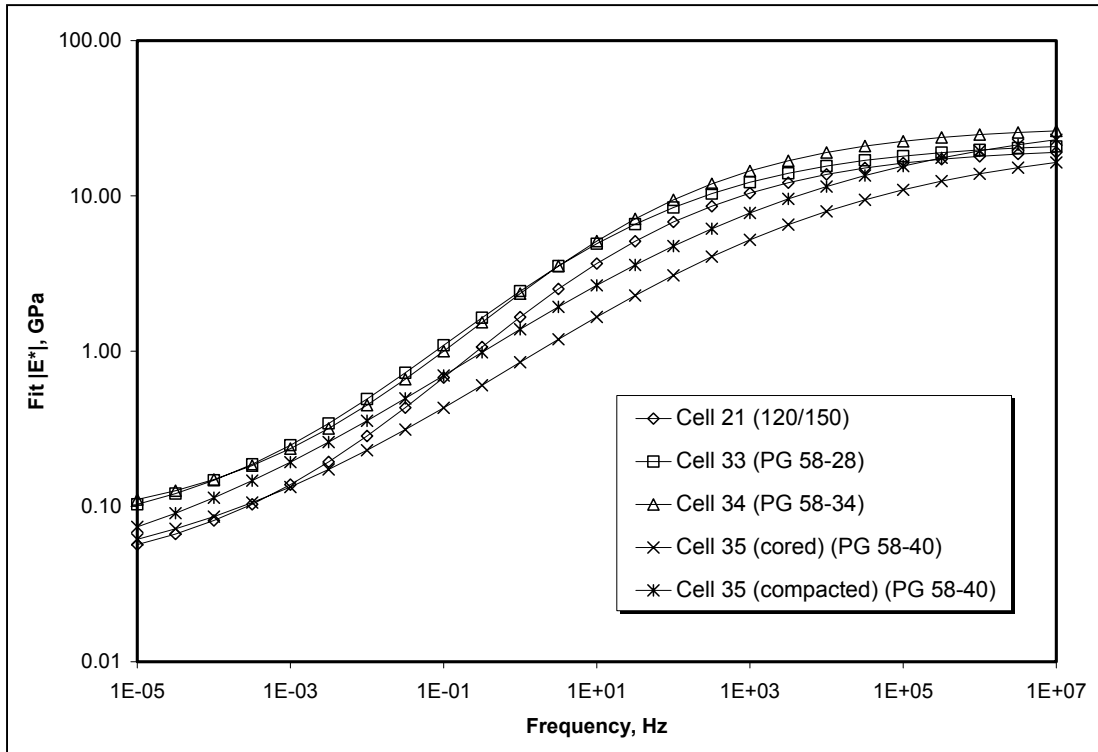


Figure 4.15. Dynamic Modulus Master Curves

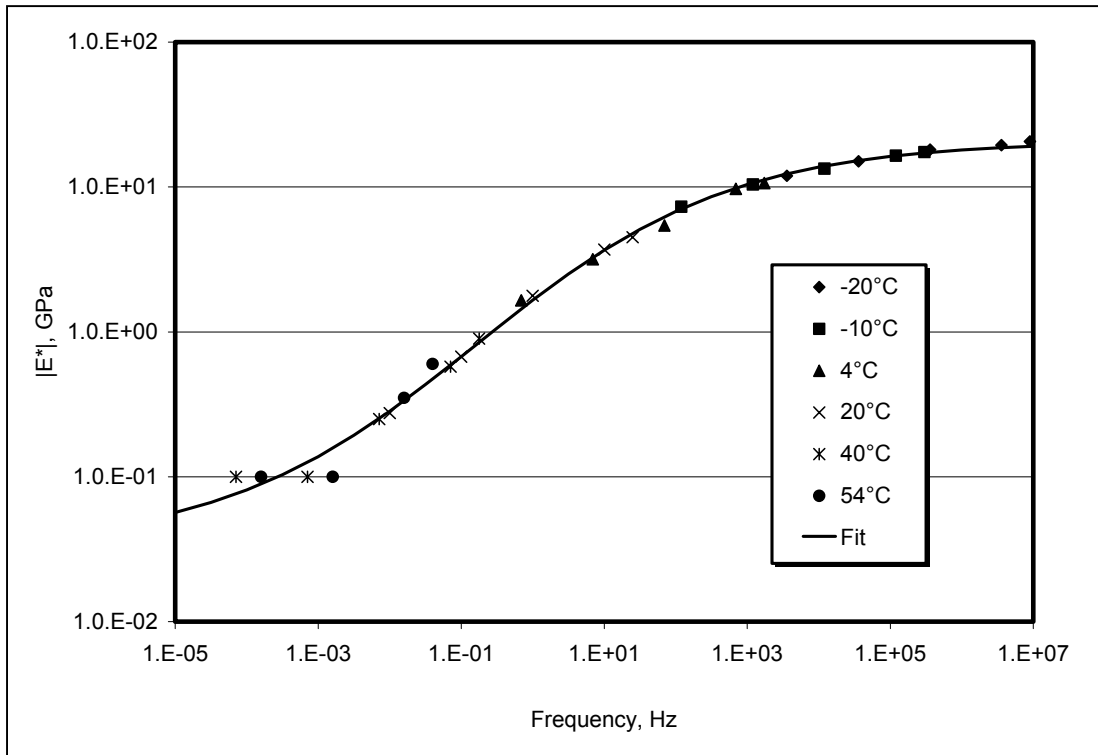


Figure 4.16. Dynamic Modulus Master Curve for Cell 21

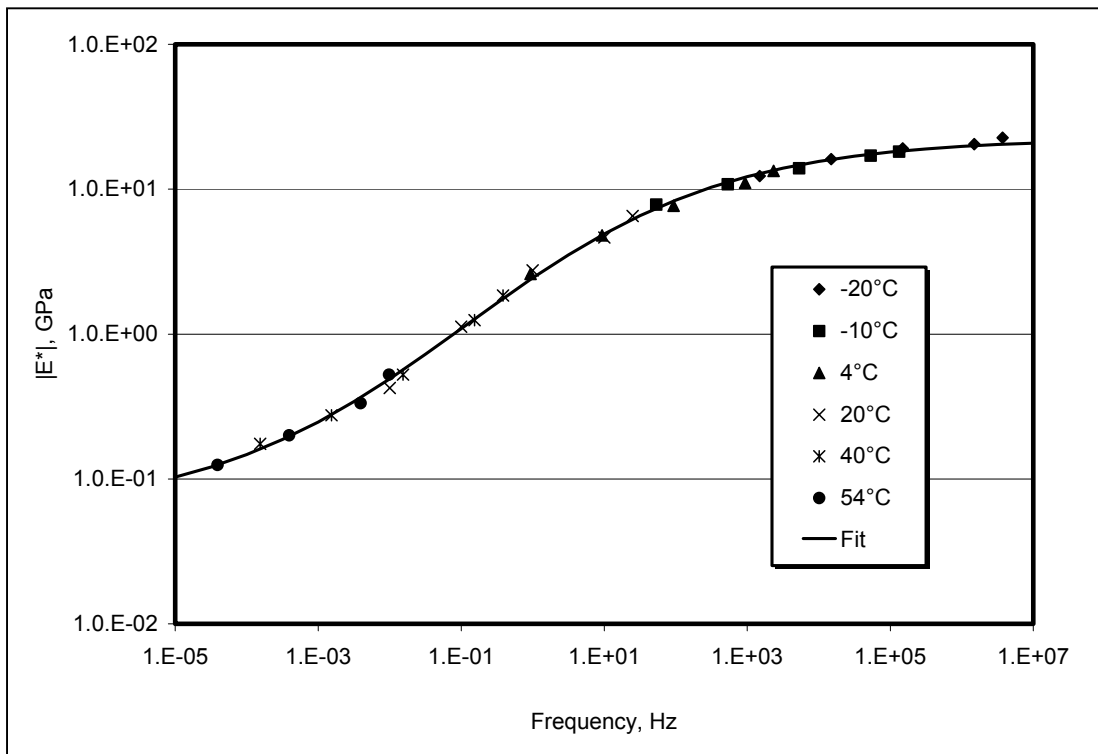


Figure 4.17. Dynamic Modulus Master Curve for Cell 33

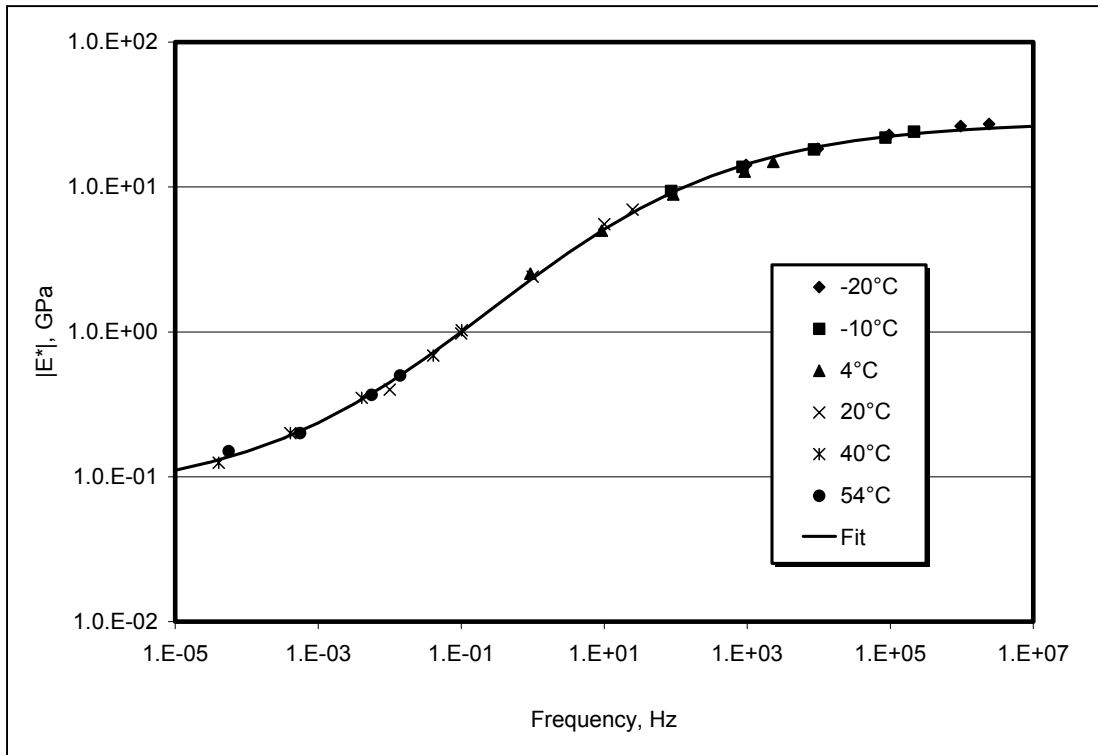


Figure 4.18. Dynamic Modulus Master Curve for Cell 34

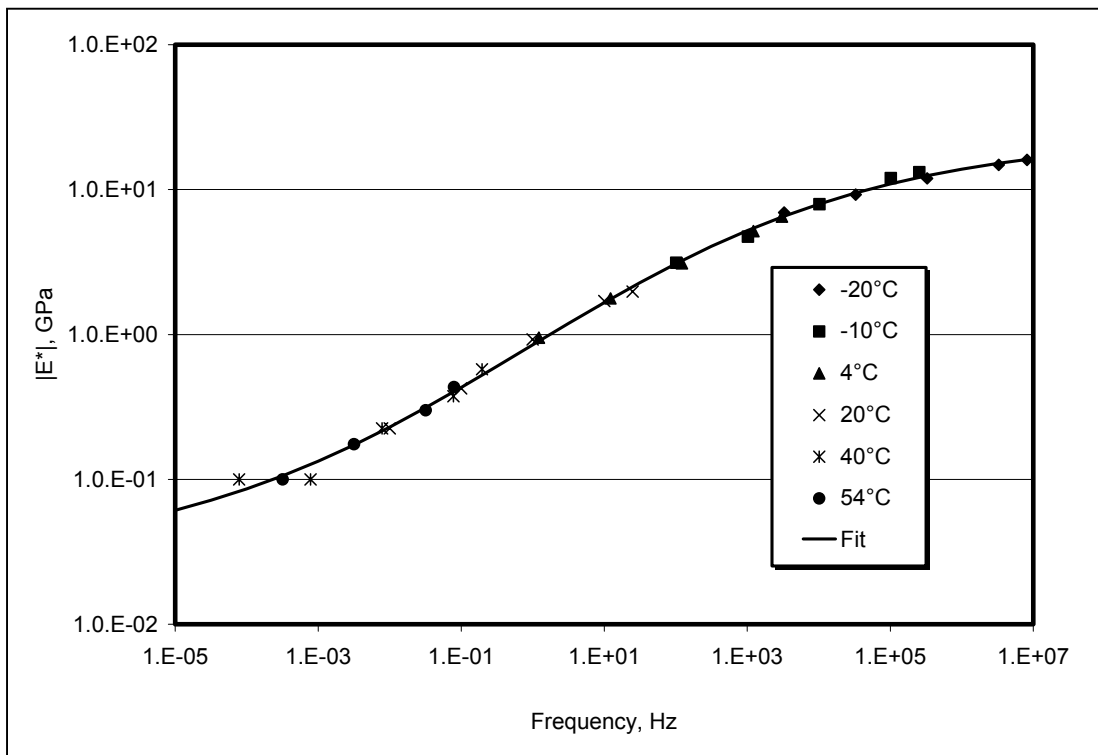


Figure 4.19. Dynamic Modulus Master Curve for Cell 35 (cored)

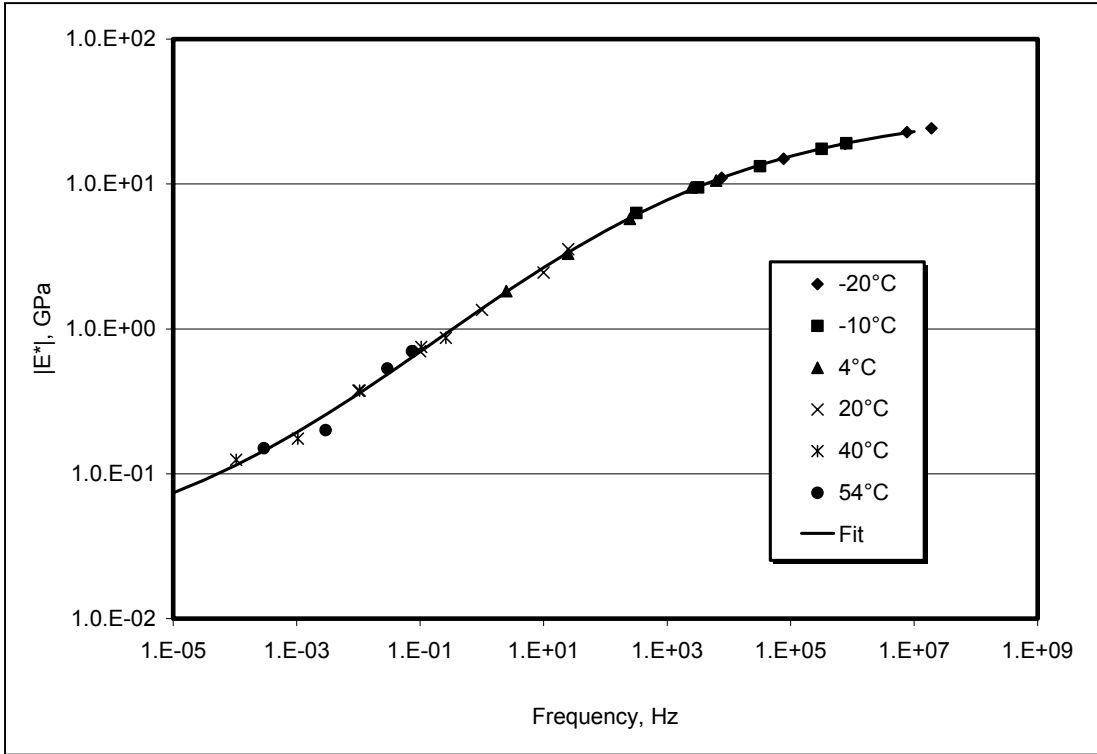


Figure 4.20. Dynamic Modulus Master Curve for Cell 35 (compacted)

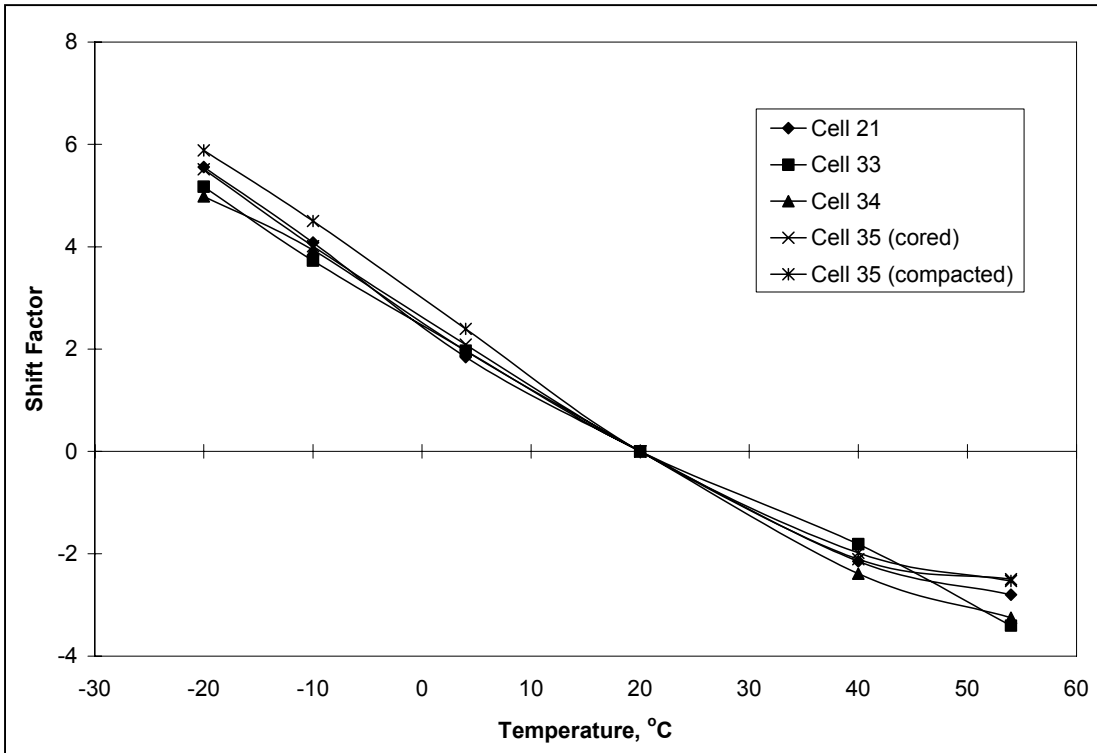


Figure 4.21. Shift Factor vs. Temperature

In constructing the master curves, the data points obtained at test temperatures above the reference are horizontally shifted to the left (lower frequencies) and the data points obtained at test temperatures below the reference temperature are shifted to the right (higher frequencies), while the data at the reference temperature remain unchanged. From the master curves for the dynamic modulus, the following observations were made:

1. In general, equation (4.14) describes the dynamic modulus quite well. In a few instances, the test data did not match predicted values for high temperatures and low frequencies.
2. There was very little difference in dynamic modulus over the entire range of frequencies between the Cell 33 and Cell 34 mixtures.
3. The two mixtures from Cell 35 had the lowest dynamic modulus values at intermediate and high temperatures. A softer asphalt was used here (PG 58-40).

The shift factors were similar for all asphalt mixtures. At 40°C and 54°C, the curves seemed slightly out of alignment. For the most part, the shift factors followed a second-order polynomial with respect to temperature. Using time-temperature superposition, master curves of dynamic modulus vs. temperature were constructed for a reference frequency of 10 Hz. These curves are shown in Figure 4.22.

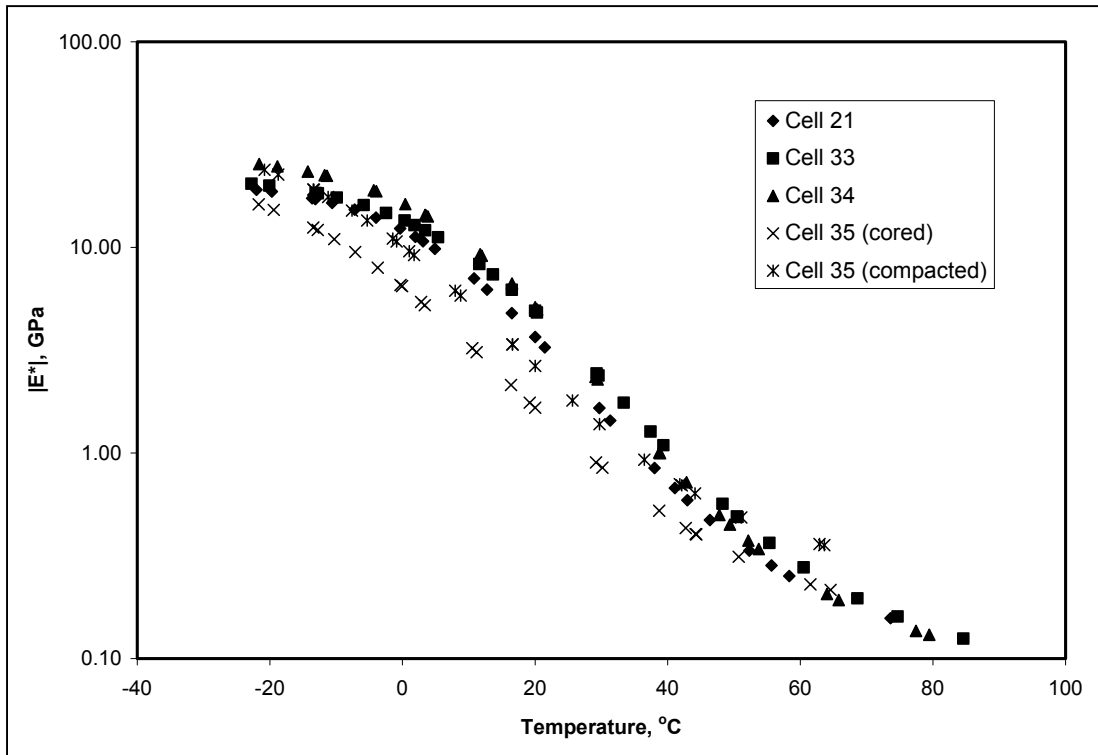


Figure 4.22. Dynamic Modulus vs. Temperature at 10 Hz

The same shift factors that were used in the construction of dynamic modulus master curves also may be used to create master curves of phase angle vs. frequency. The shift factor was applied for each mixture, and the phase angle was plotted against the shifted frequency. These plots are shown in Figures 4.23 to 4.26.

The plots indicate that none of the phase angle master curves are smooth. The data appears scattered especially at the higher test temperatures. At low temperatures, the phase angle master curves appeared relatively smooth. As expected, the phase angle follows the behavior of a viscoelastic material; i. e., it decreases as the frequency increases, except at the higher test temperatures, where the phase angle decreases with a decrease in frequency as a consequence of aggregate interlock effects.

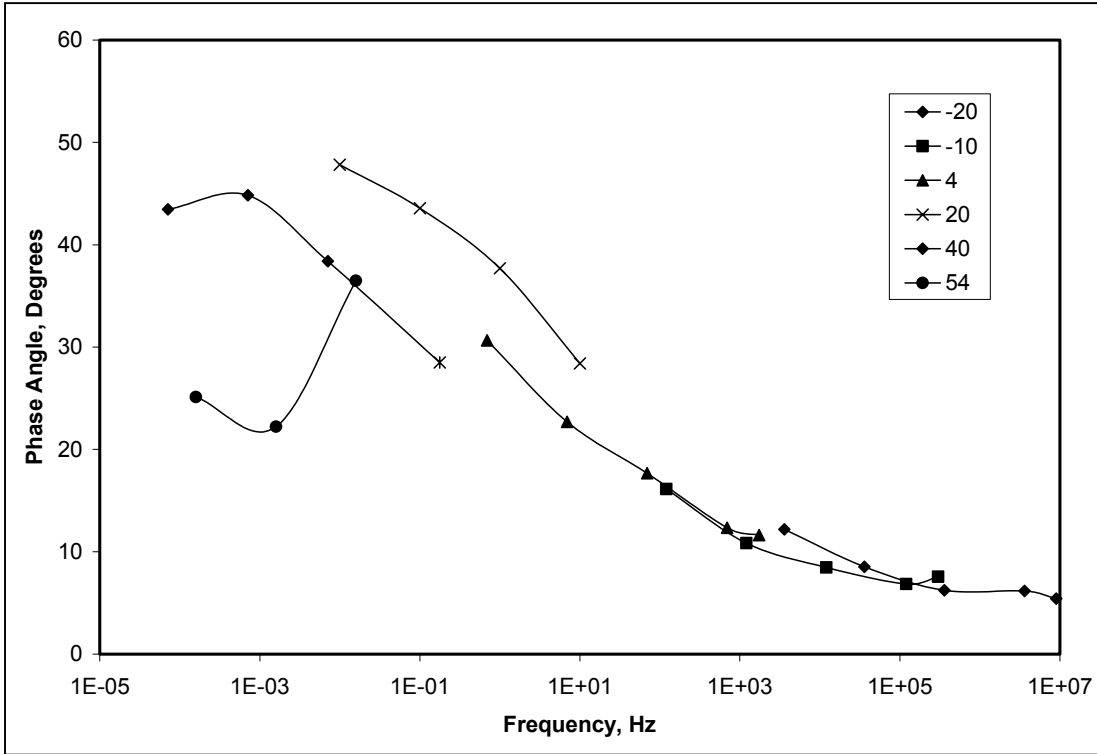


Figure 4.23. Phase Angle Master Curve for Cell 21

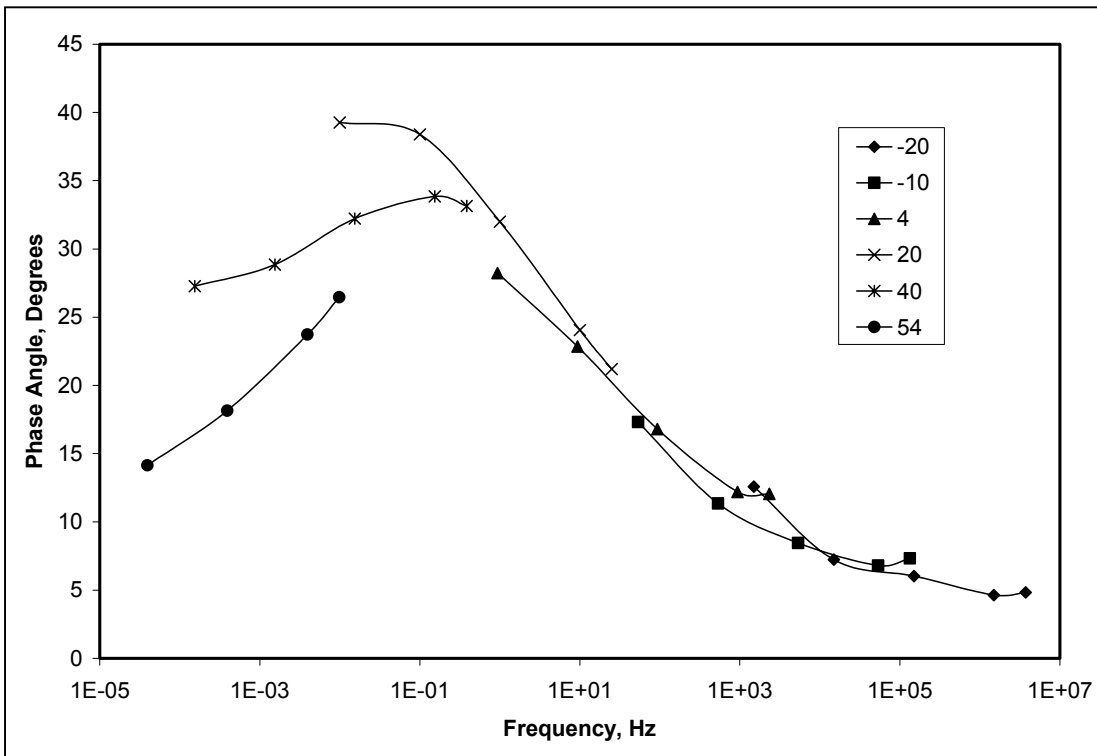


Figure 4.24. Phase Angle Master Curve for Cell 33

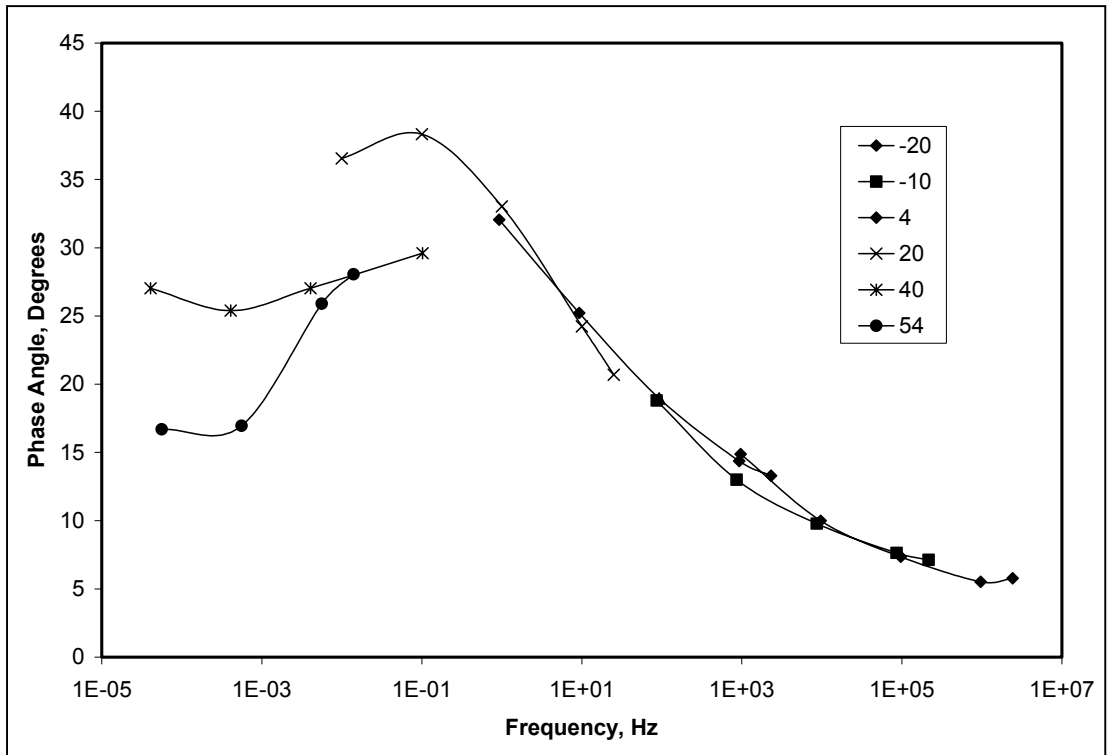


Figure 4.25. Phase Angle Master Curve for Cell 34

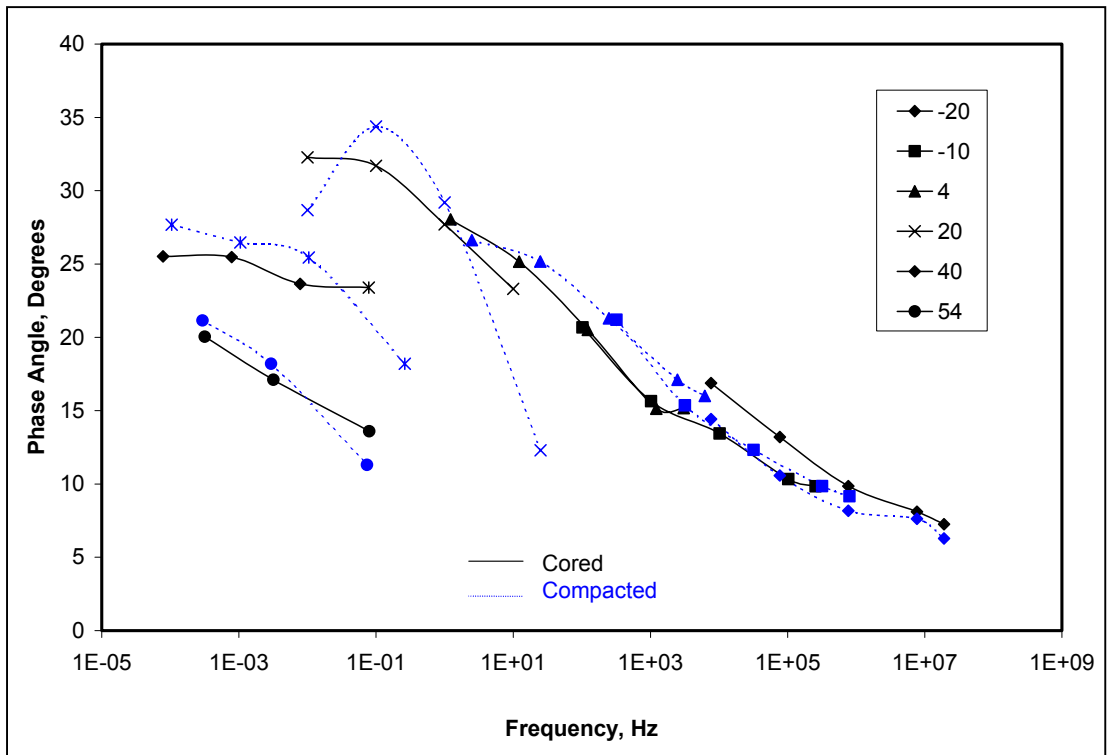


Figure 4.26. Phase Angle Master Curve for Cell 35

Predictive Equations

The dynamic complex modulus test is relatively difficult and expensive to perform. A predictive equation proposed as part of the 2002 Design Guide [15] calculates $|E^*|$ based on the properties of its components.

The first model was developed in 1995 at the University of Maryland and takes into account the hardening effects that take place during short- and long-term aging [21]:

$$\log|E^*| = -0.261 + 0.008225P_{200} - 0.00000101(P_{200})^2 + 0.00196P_4 - 0.03157V_a - 0.415 \frac{V_{beff}}{(V_{beff} + V_a)} + \frac{[1.87 + 0.002808P_4 + 0.00000404P_{38} - 0.0001786(P_{38})^2 + 0.0164P_{34}]}{1 + e^{(-0.716 \log f - 0.7425 \log \eta)}} \quad (4.15)$$

where

$|E^*|$ = asphalt mix dynamic modulus, in 10^5 psi;

η = bitumen viscosity, in 10^6 poise;

f = load frequency, in Hz;

V_a = percent air voids in the mix, by volume;

V_{beff} = percent effective bitumen content, by volume;

P_{34} = percent retained on $\frac{3}{4}$ -in. (19-mm) sieve, by total aggregate weight (cumulative);

P_{38} = percent retained on $\frac{3}{8}$ -in. (9-mm) sieve, by total aggregate weight (cumulative);

P_4 = percent retained on #4 (4.75-mm) sieve, by total aggregate weight (cumulative); and

P_{200} = percent passing #200 (0.075-mm) sieve, by total aggregate weight.

The above predictive equation was developed from 2,750 specimens for 205 different asphalt mixtures using regression techniques. Notice that this equation has a similar form with equation (4.14). The fitting parameters δ and α are calculated as a function of the component properties.

In 2000, the predictive equation for the complex dynamic modulus was modified as shown below:

$$\log|E^*| = -1.249937 + 0.029232P_{200} - 0.001767(P_{200})^2 + 0.002841P_4 - 0.058097V_a - 0.802208 \frac{V_{beff}}{(V_{beff} + V_a)} + \frac{[3.871977 - 0.0021P_4 + 0.003958P_{38} - 0.000017(P_{38})^2 + 0.00547P_{34}]}{1 + e^{(-0.603313 - 0.313351 \log f - 0.393532 \log \eta)}} \quad (4.16)$$

This equation uses the same parameters as equation (4.15). The equation's form did not change; only the coefficients are changed to reflect calibration to more data.

In this research project the modulus was calculated using both equations (4.15) and (4.16). Gradation data for each mixture, as well as binder content, were obtained from the Job Mix Formulas provided by Mn/DOT. The air voids were measured using test method AASHTO T 166 on the prepared test specimens. The binder viscosity was calculated at each temperature using Dynamic Shear Rheometer results provided by Mn/DOT. The following tables show the dynamic modulus in GPa calculated from equations (4.15) and (4.16).

Table 4.8. Cell 21 Dynamic Modulus from Witczak 1995 Model

| <i>Mn/ROAD Cell 21 120/150</i> | | | | | |
|--------------------------------|---------------|-------|-------|-------|-------|
| Temp. °C | Frequency, Hz | | | | |
| | 0.01 | 0.1 | 1 | 10 | 25 |
| -20 | 13.01 | 13.75 | 14.14 | 14.34 | 14.38 |
| -10 | 8.26 | 10.82 | 12.51 | 13.49 | 13.74 |
| 4 | 1.61 | 3.44 | 6.25 | 9.21 | 10.22 |
| 20 | 0.36 | 0.62 | 1.30 | 2.83 | 3.75 |
| 40 | 0.21 | 0.25 | 0.35 | 0.61 | 0.80 |
| 54 | 0.19 | 0.21 | 0.25 | 0.34 | 0.41 |

Table 4.9. Cell 33 Dynamic Modulus from Witczak 1995 Model

| <i>Mn/ROAD Cell 33 PG 58-28</i> | | | | | |
|---------------------------------|---------------|-------|-------|-------|-------|
| Temp. °C | Frequency, Hz | | | | |
| | 0.01 | 0.1 | 1 | 10 | 25 |
| -20 | 12.65 | 13.55 | 14.02 | 14.26 | 14.32 |
| -10 | 7.57 | 10.29 | 12.18 | 13.29 | 13.58 |
| 4 | 1.42 | 3.09 | 5.78 | 8.77 | 9.83 |
| 20 | 0.34 | 0.58 | 1.20 | 2.64 | 3.52 |
| 40 | 0.21 | 0.25 | 0.34 | 0.59 | 0.77 |
| 54 | 0.19 | 0.20 | 0.24 | 0.34 | 0.41 |

Table 4.10. Cell 34 Dynamic Modulus from Witczak 1995 Model

| <i>Mn/ROAD Cell 34 PG 58-34</i> | | | | | |
|---------------------------------|---------------|------|-------|-------|-------|
| Temp. °C | Frequency, Hz | | | | |
| | 0.01 | 0.1 | 1 | 10 | 25 |
| -20 | 5.92 | 9.04 | 11.56 | 13.18 | 13.62 |
| -10 | 2.03 | 4.21 | 7.26 | 10.21 | 11.17 |
| 4 | 0.54 | 1.08 | 2.38 | 4.80 | 6.01 |
| 20 | 0.27 | 0.39 | 0.70 | 1.48 | 2.03 |
| 40 | 0.21 | 0.24 | 0.32 | 0.51 | 0.65 |
| 54 | 0.19 | 0.21 | 0.25 | 0.34 | 0.40 |

Table 4.11. Cell 35 (cored) Dynamic Modulus from Witzak 1995 Model

| <i>Mn/ROAD Cell 35 PG 58-40(cored)</i> | | | | | |
|--|---------------|------|------|------|-------|
| Temp. °C | Frequency, Hz | | | | |
| | 0.01 | 0.1 | 1 | 10 | 25 |
| -20 | 1.72 | 3.66 | 6.57 | 9.57 | 10.58 |
| -10 | 0.77 | 1.66 | 3.55 | 6.43 | 7.67 |
| 4 | 0.37 | 0.66 | 1.38 | 3.00 | 3.96 |
| 20 | 0.25 | 0.35 | 0.59 | 1.22 | 1.67 |
| 40 | 0.21 | 0.24 | 0.33 | 0.54 | 0.70 |
| 54 | 0.19 | 0.22 | 0.27 | 0.38 | 0.47 |

Table 4.12. Cell 21 Dynamic Modulus from Witzak 2000 Model

| <i>Mn/ROAD Cell 21 120/150</i> | | | | | |
|--------------------------------|---------------|-------|-------|-------|-------|
| Temp. °C | Frequency, Hz | | | | |
| | 0.01 | 0.1 | 1 | 10 | 25 |
| -20 | 23.35 | 27.02 | 30.15 | 32.74 | 33.62 |
| -10 | 11.18 | 15.27 | 19.51 | 23.56 | 25.07 |
| 4 | 2.37 | 4.20 | 6.86 | 10.31 | 11.85 |
| 20 | 0.38 | 0.75 | 1.48 | 2.75 | 3.46 |
| 40 | 0.08 | 0.14 | 0.27 | 0.54 | 0.72 |
| 54 | 0.04 | 0.07 | 0.12 | 0.22 | 0.29 |

Table 4.13. Cell 33 Dynamic Modulus from Witzak 2000 Model

| <i>Mn/ROAD Cell 33 PG 58-28</i> | | | | | |
|---------------------------------|---------------|-------|-------|-------|-------|
| Temp. °C | Frequency, Hz | | | | |
| | 0.01 | 0.1 | 1 | 10 | 25 |
| -20 | 20.39 | 23.96 | 27.07 | 29.67 | 30.56 |
| -10 | 9.44 | 13.15 | 17.09 | 20.94 | 22.39 |
| 4 | 1.98 | 3.55 | 5.88 | 8.97 | 10.38 |
| 20 | 0.33 | 0.65 | 1.28 | 2.41 | 3.03 |
| 40 | 0.07 | 0.13 | 0.24 | 0.49 | 0.64 |
| 54 | 0.04 | 0.06 | 0.11 | 0.21 | 0.27 |

Table 4.14. Cell 34 Dynamic Modulus from Witzak 2000 Model

| <i>Mn/ROAD Cell 34 PG 58-34</i> | | | | | |
|---------------------------------|---------------|-------|-------|-------|-------|
| Temp. °C | Frequency, Hz | | | | |
| | 0.01 | 0.1 | 1 | 10 | 25 |
| -20 | 7.48 | 11.05 | 15.11 | 19.33 | 20.97 |
| -10 | 2.82 | 4.88 | 7.77 | 11.40 | 12.99 |
| 4 | 0.69 | 1.36 | 2.55 | 4.47 | 5.46 |
| 20 | 0.18 | 0.36 | 0.72 | 1.41 | 1.83 |
| 40 | 0.06 | 0.11 | 0.20 | 0.40 | 0.53 |
| 54 | 0.04 | 0.06 | 0.11 | 0.20 | 0.27 |

Table 4.15. Cell 35 (cored) Dynamic Modulus from Witczak 2000 Model

| <i>Mn/ROAD Cell 35 PG 58-40(cored)</i> | | | | | |
|--|---------------|------|------|-------|-------|
| Temp. °C | Frequency, Hz | | | | |
| | 0.01 | 0.1 | 1 | 10 | 25 |
| -20 | 2.41 | 4.23 | 6.87 | 10.27 | 11.78 |
| -10 | 1.07 | 2.05 | 3.67 | 6.09 | 7.28 |
| 4 | 0.38 | 0.76 | 1.49 | 2.77 | 3.48 |
| 20 | 0.15 | 0.29 | 0.58 | 1.15 | 1.49 |
| 40 | 0.06 | 0.12 | 0.22 | 0.44 | 0.58 |
| 54 | 0.04 | 0.07 | 0.13 | 0.26 | 0.34 |

The data in Tables 4.8 to 4.15 were used to develop dynamic complex modulus master curves. Comparisons were made between data obtained from the laboratory tests and the values calculated from equations (4.15) and (4.16). The following figures show these comparisons for all five mixtures.

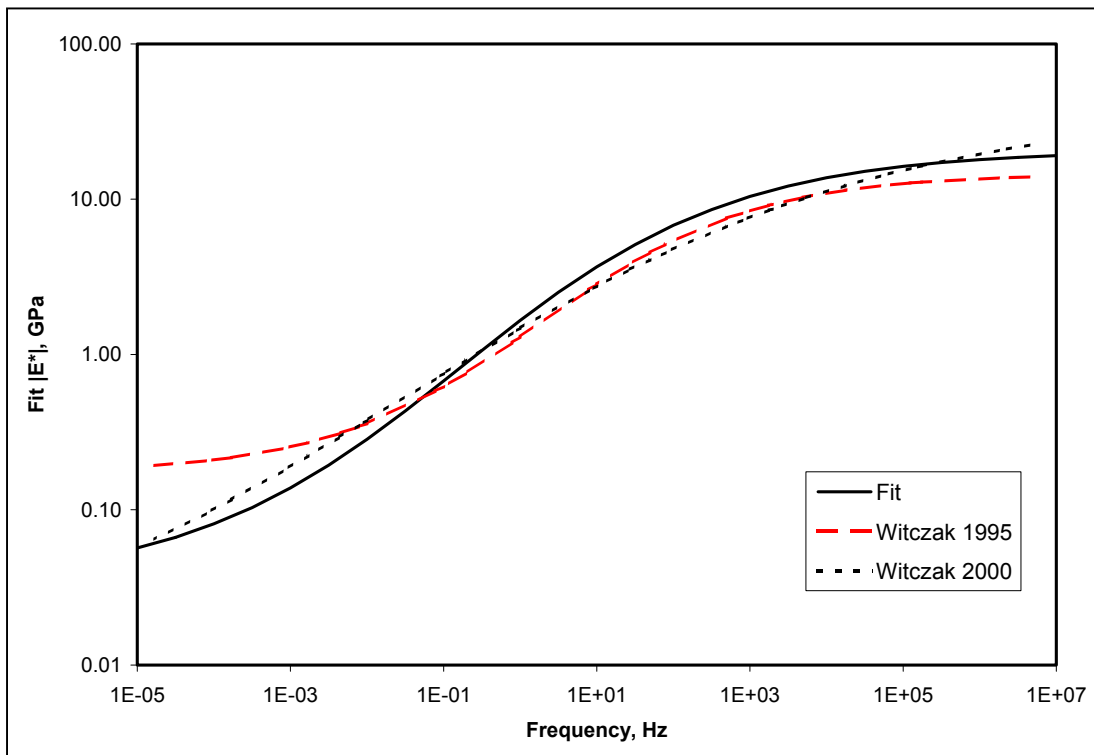


Figure 4.27. Master Curve Comparison (Cell 21)

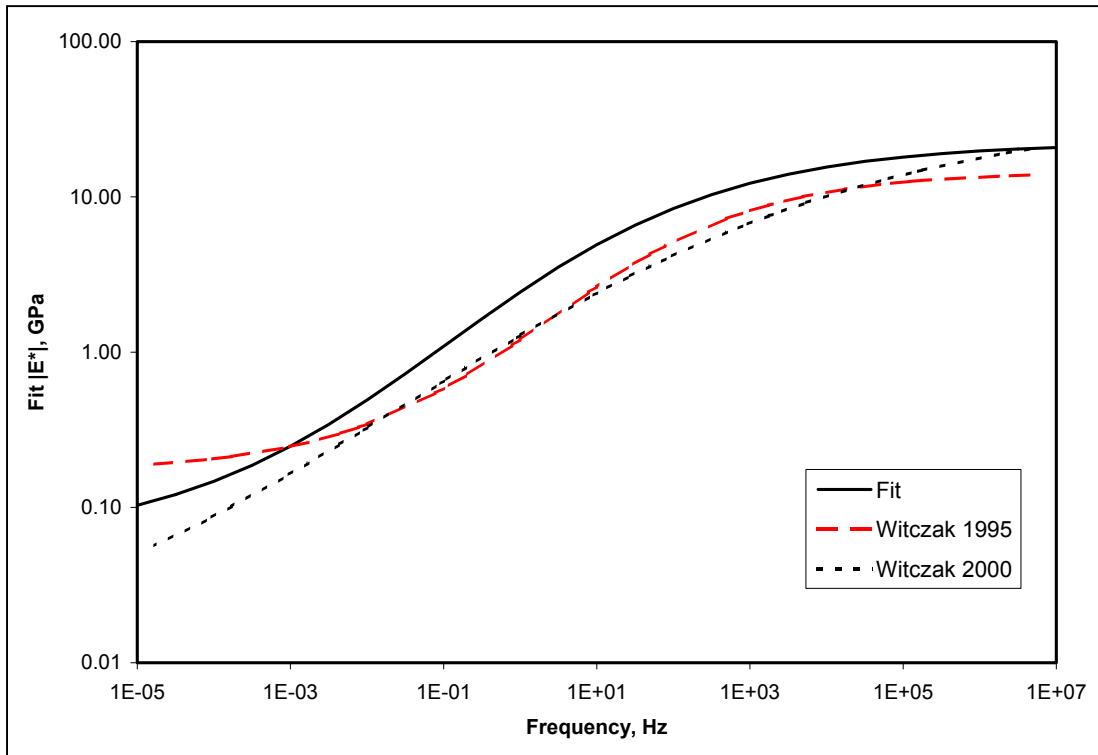


Figure 4.28. Master Curve Comparison (Cell 33)

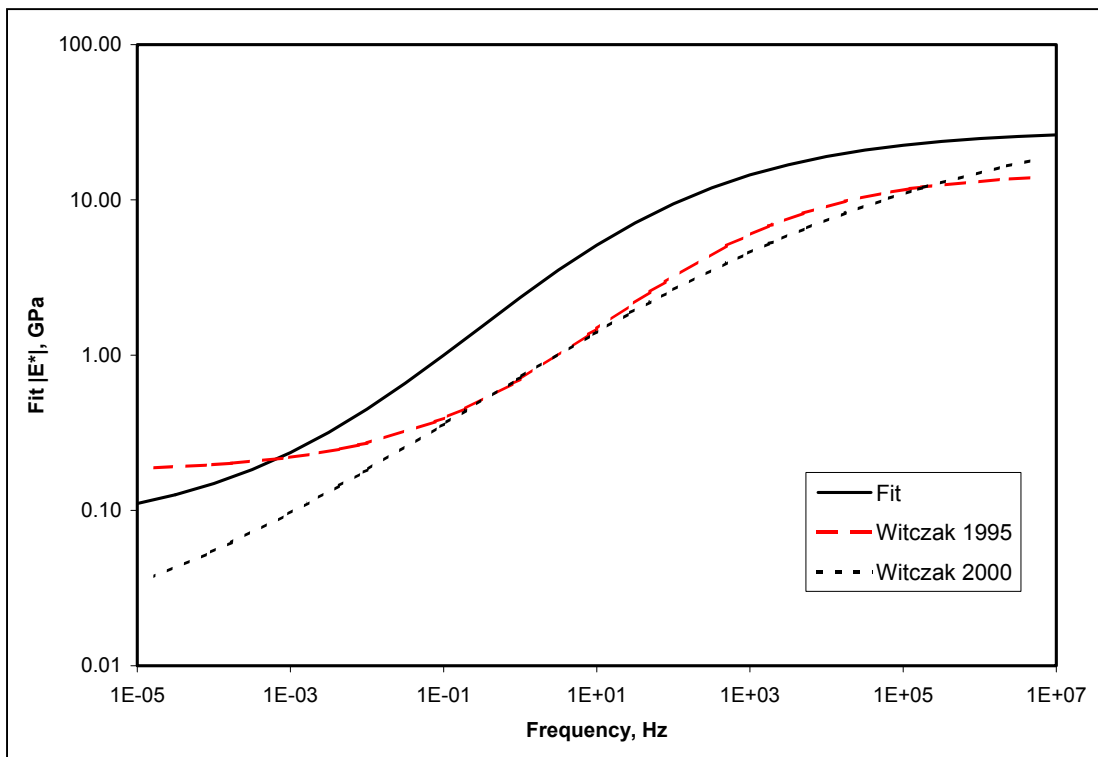


Figure 4.29. Master Curve Comparison (Cell 34)

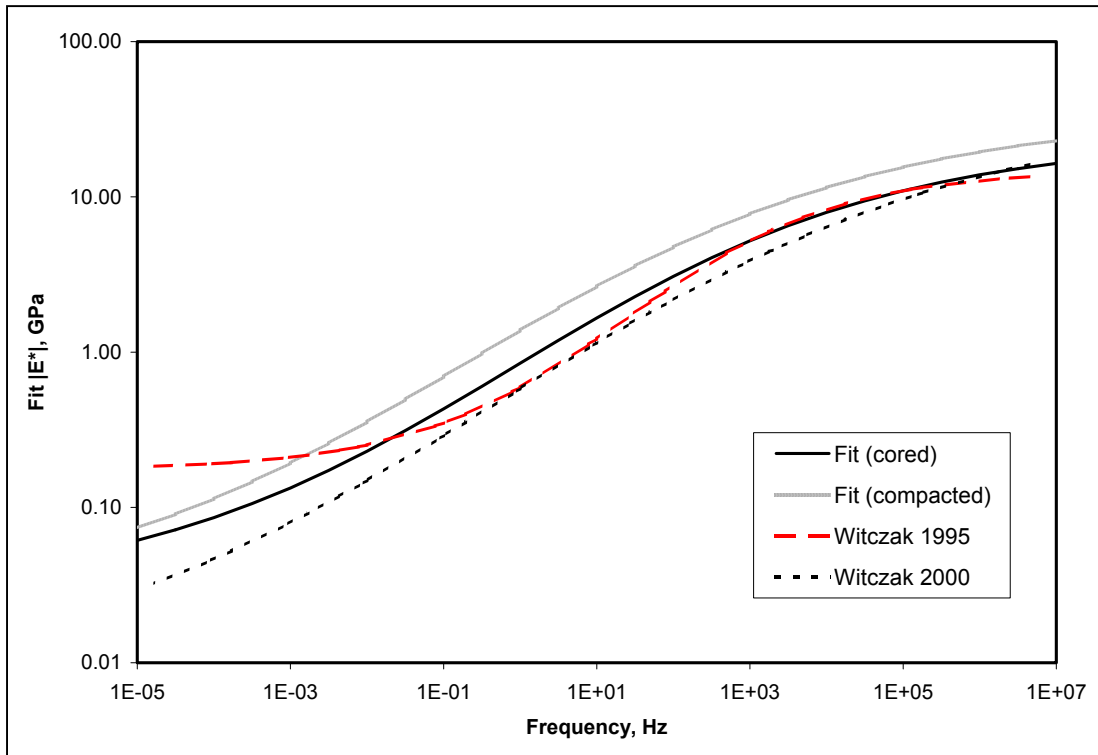


Figure 4.30. Master Curve Comparison (Cell 35)

From the above master curves, the following observations were made:

1. For the mixtures from Cells 21 and 35, the predictive equations fit the test data relatively well at intermediate and low temperatures. At high temperatures, the predictive equations tend to drift away from the test data.
2. For the mixtures from Cells 33 and 34, the predictive equations do not fit the test data very well.
3. For all five mixtures, the test data is generally larger than the predicted value of dynamic complex modulus.
4. The 2000 predictive equation tends to fit the shape of the test data master curve better than the 1995 equation. The latter equation has a more pronounced “s” shape, while the 2000 equation projects a flatter curve.

Chapter 5

Vibration Testing

Introduction

This chapter summarizes a preliminary evaluation of a vibration tester used to measure the complex modulus of asphalt mixtures. This technique uses less expensive equipment than traditional complex modulus testing and is easier to perform. The results from this testing are compared to $|E^*|$ data obtained using NCHRP 9-29 protocols for one of the asphalt mixtures evaluated in this project.

Materials

The objective of this preliminary evaluation was to obtain the dynamic modulus of one asphalt mixture from Mn/ROAD using a simple vibration test. The mixture selected for this study was from Cell 35. Two samples that previously were tested with the NCHRP 9-29 protocol were retested with the vibration exciter. Table 5.1 shows the mixture's basic properties, Table 5.2 shows the mixture gradation, and Table 5.3 shows the parameters obtained during sample preparation.

Table 5.1. Material Properties

| | |
|--------------------------|-------------|
| Cell | 35 |
| Binder Type | PG 58-40 |
| Polymer Modified? | Yes |
| Sample Type | Loose Mix |
| Paving Date | August 1999 |

Table 5.2. Mixture Gradations

| Sieve Size, mm | Sieve Size, in. | Percent Passing |
|----------------|-----------------|-----------------|
| 19 | 3/4 | 100 |
| 12.5 | 1/2 | 94 |
| 9.0 | 3/8 | 86 |
| 4.75 | #4 | 66 |
| 2.36 | #8 | 54 |
| 0.075 | #200 | 4.7 |

Table 5.3. Sample Preparation Data

| Cell | Sample # | Compaction Temperature, °C | # Gyations | Air Voids | Height, mm | Diameter, mm |
|------|----------|----------------------------|------------|-----------|------------|--------------|
| 35 | 58-40-1 | 124 | 40 | 4.8% | 146.98 | 100.58 |
| 35 | 58-40-4 | 124 | 40 | 4.8% | 155.05 | 100.61 |

Testing Equipment

The Vibration Exciter Type 4809, made by Brüel & Kjær in Denmark, was the device used for the vibration testing. Driven by a small power amplifier, it uses vibration transducers to measure deformation. A permanent magnet drives the moving element inside to apply load to the specimen. A threaded insert is set into the table surface for attachment purposes. The device weighs about 20 lbs. (9 kg) and its dimensions are 6 in. (150 mm) in diameter by 6 in. (150 mm) in height. Figure 5.1 shows a schematic of the 4809 Exciter.

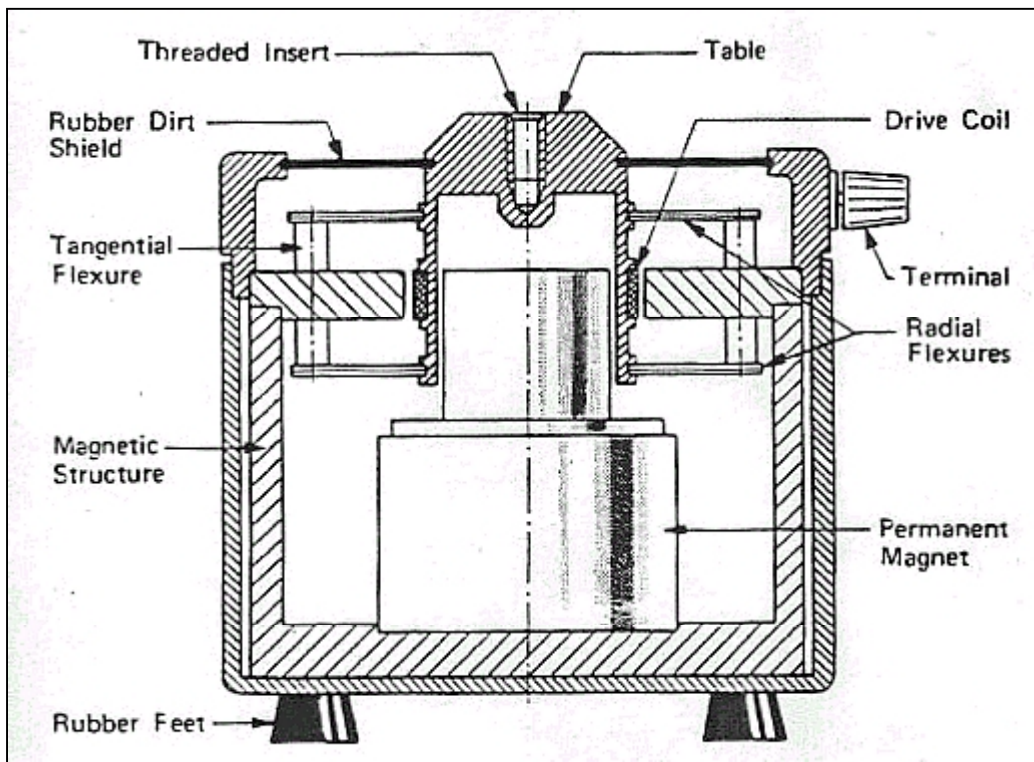


Figure 5.1. Vibration Exciter Type 4809

Test Setup

All tests were performed inside an environmental chamber (Thermotron Industries Model # FR-3-CH-LN2). Liquid nitrogen tanks were used to cool the chamber below room temperature, and mechanical heating was used to reach 40°C. The temperature was controlled by an MTS 409.80 Temperature Controller, and verified by using an independent Omega 869C platinum RTD thermometer.

The test specimen was placed in a frame inside the environmental chamber. A thick aluminum plate was mounted onto the 4809 Exciter via the fixing hole at the center of the vibration table. Another aluminum plate was glued to this plate to provide uniform axial stress to the test specimen. The Exciter was then flipped upside down and placed on top of the test specimen inside the chamber. Three rubber feet extended down from the exciter to rest on the load frame to relieve the weight of the exciter from the specimen. A thin layer of Vaseline was spread on top of the specimen to ensure good contact between the specimen and the aluminum plate. Figure 5.2 shows the test setup.



Figure 5.2. Vibration Test Setup

Testing Procedures

Vibration tests were performed at temperatures of 5, 20, and 40°C per equipment specifications. Testing began with the lowest temperature and proceeded to the highest. A frequency sweep from 1 to 100 Hz was performed at each temperature. A load cell measured the force and two accelerometers measured acceleration resulting from the vibration. The data from the accelerometers was integrated twice to obtain displacement measurements. Data below about 35 Hz was quite erratic, so it was eliminated. The remaining data allowed for construction of dynamic modulus master curves over a wide range of frequencies.

Testing Results

The testing program collected the raw data, and a simple MatLab program analyzed the data. The force and displacement measurements were used to calculate the complex modulus at each frequency. Figures 5.3 and 5.4 show the complex modulus vs. frequency for samples 1 and 4, respectively.

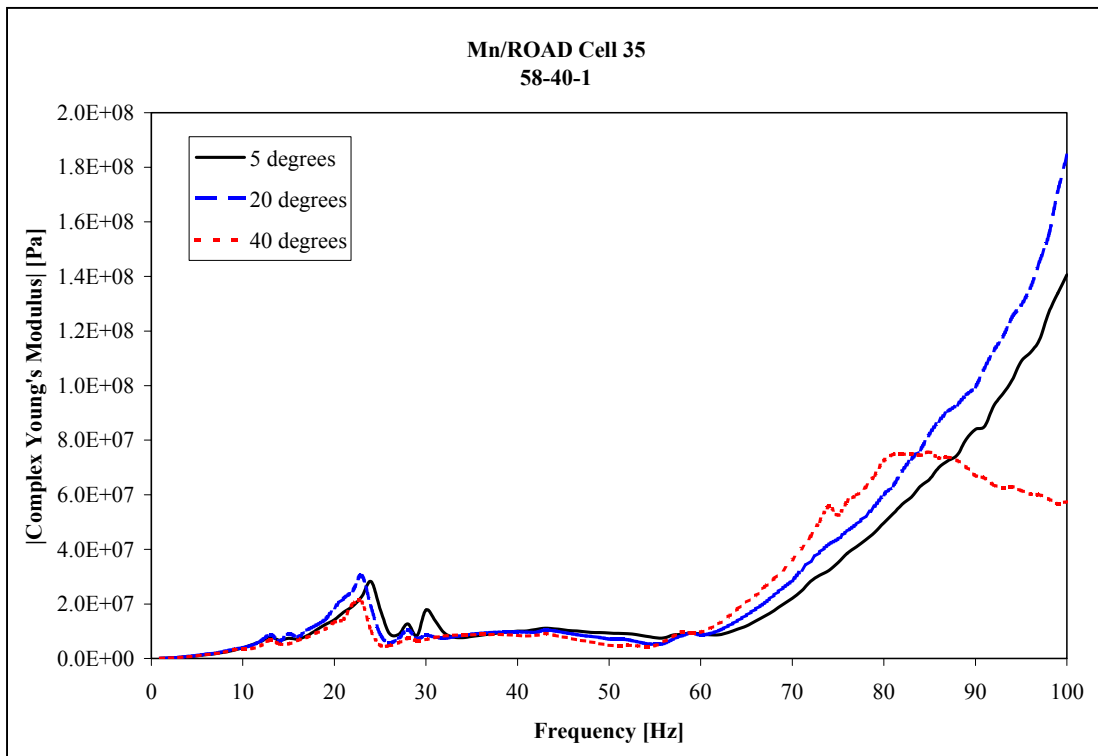


Figure 5.3. Vibration Test Results for Sample 58-40-1

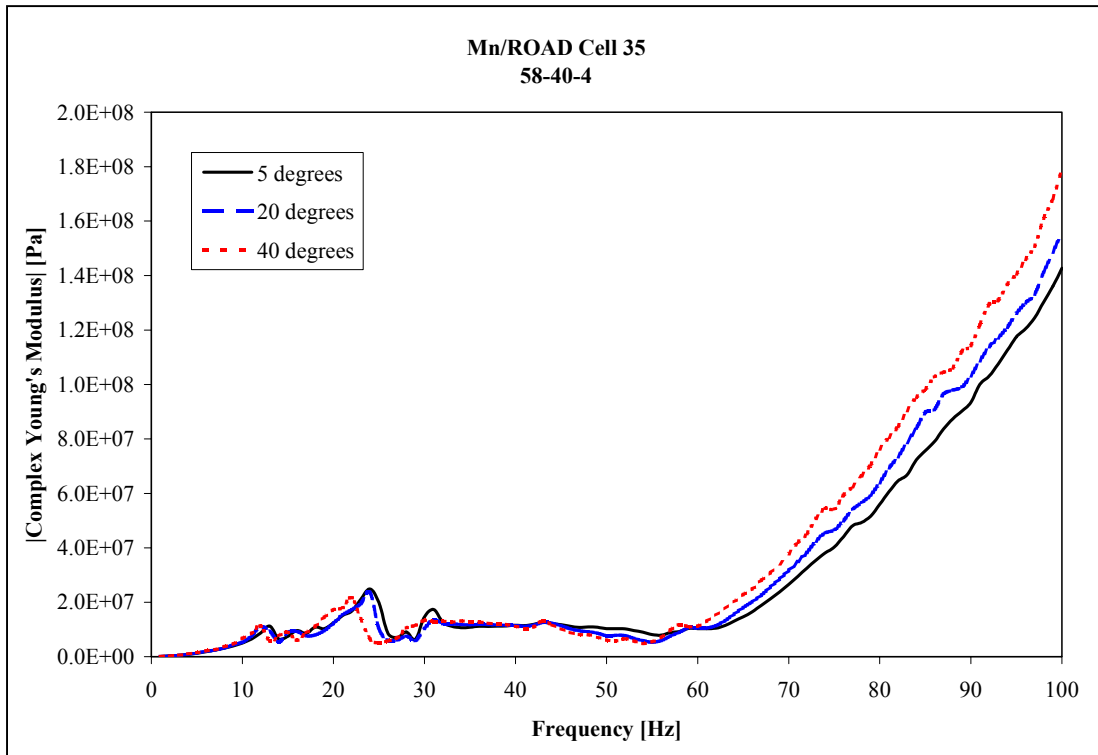


Figure 5.4. Vibration Test Results for Sample 58-40-4

Data Analysis

The limited results show that the dynamic complex modulus values obtained with the vibration method are not reliable. The shape of the frequency sweep data is not smooth and up to 60 Hz it does not vary with the change in frequency, which is unrealistic. The maximum modulus values obtained were less than 200 MPa. In addition the temperature effect is almost insignificant and on a log scale the three temperatures are undistinguishable from each other. Normal scale plots reveal that the temperature effect is the opposite of what was expected: The lower temperature had slightly lower modulus values than the higher temperatures, which again is unrealistic.

Based on these preliminary results, further investigation of the characterization of asphalt mixtures using the vibration method was abandoned.

Chapter 6

Conclusions and Recommendations

Conclusions

In this project the dynamic modulus and phase angle values were determined for four Minnesota asphalt mixtures. Twenty specimens from four mixtures were tested under six temperatures and five frequencies. Based on the test data, master curves for each mixture were constructed, and the validity of Witczak's predictive equations was evaluated. The following conclusions can be drawn from the tests:

1. Under a constant load frequency, the dynamic modulus decreases with the increase in test temperature for the same mixture, while the phase angle increases with the increase in test temperature from -20°C to 20°C. However, at 40°C and 54°C the phase angle decreases with the increase in test temperature, as expected.
2. Under a constant test temperature, the dynamic modulus increases with the increase of test frequency and the phase angle generally shows the opposite trend, as expected.
3. Use of the same shift factors as for the complex modulus master curves did not result in smooth master curves for the phase angle.
4. The modulus values calculated using the 2000 predictive equation are reasonably close to the experimental values obtained for the mixtures from Cells 21 and 35. However, for the mixtures from Cells 33 and 34, the differences are significant.
5. As expected, the softest asphalt (PG 58-40) had the lowest dynamic modulus. The mixtures with stiffer asphalts (PG 58-28 and PG 58-34) had higher dynamic modulus values.
6. Sample preparation techniques do affect the results of dynamic modulus testing. The recommended procedure of coring and cutting test specimens led to a lower modulus than that of specimens compacted directly to size for the mixture investigated.
7. The limited results show that the dynamic complex modulus values obtained with the vibration method are not reliable. The dynamic modulus values at three different temperatures are almost indistinguishable. Furthermore, the highest test temperature yielded the highest modulus, which is opposite to what is expected.

Recommendations

1. The use of complex modulus as a design parameter and simple performance test should be further investigated. More tests should be performed on mixtures obtained from Mn/ROAD cells or other pavements for which performance data is available.
2. Testing equipment should be upgraded to provide multiple extensometer measurements. The current configuration uses two extensometers that are averaged together to obtain one output strain.
3. The 2000 predictive equation should be used with caution. The equation provided a reasonable prediction of the dynamic modulus for two of the four mixtures evaluated. Further research is needed to validate the predictive equation for asphalt mixtures typically used in Minnesota. A sensitivity study that investigates the influence of the different parameters used in the predictive equation on the modulus value should be performed as a next step.
4. Further investigation of a vibration device to measure complex modulus should be undertaken. Vibration tests under the current study were minimal, as was the data analysis tools used. Additional research could prove beneficial in using a lower-cost device to perform complex modulus tests.

References

1. Papazian, H. S., "The Response of Linear Viscoelastic Materials in the Frequency Domain with Emphasis on Asphaltic Concrete," (*1st*) *International Conference on the Structural Design of Asphalt Pavements*, 1962, pp. 454-463.
2. Witczak, M. W., and R. E. Root, "Summary of Complex Modulus Laboratory Test Procedures and Results," *STP 561*, American Society for Testing and Materials, 1974, pp. 67-94.
3. Khanal, P. P., and M. S. Mamlouk, "Tensile Versus Compressive Moduli of Asphalt Concrete," *Transportation Research Record 1492*, 1995, pp. 144-150.
4. Bonnaure, F., Gest, G., Gravois, A., and P. Uge, "A New Method of Predicting the Stiffness of Asphalt Paving Mixtures," *Proceedings, Association of Asphalt Paving Technologists*, Vol. 46, 1977, pp. 64-100.
5. Francken, L., Partl, M., and Technical Committee on Bitumen and Asphalt Testing, "Complex Modulus Testing of Asphaltic Concrete: RILEM Interlaboratory Test Program," *Transportation Research Record 1545*, 1996, pp. 133-142.
6. Stroup-Gardiner, M., and D. E. Newcomb, "Investigation of Hot Mix Asphalt Mixtures at MnROAD," Minnesota Department of Transportation Final Report 97-06, 1997.
7. Drescher, A., Newcomb, D. E., and W. Zhang, "Interpretation of Indirect Tension Test Based on Viscoelasticity," *Transportation Research Record 1590*, 1997, pp. 45-52.
8. Zhang, W., Drescher, A., and D. E. Newcomb, "Viscoelastic Behavior of Asphalt Concrete in Diametral Compression," *Journal of Transportation Engineering*, November/December 1997, pp. 495-502.
9. Romero, P., and R. M. Anderson, "Variability of Asphalt Mixtures Tests Using the Superpave Shear Tester Repeated Shear at Constant Height Test," *Transportation Research Record 1767*, 2001, pp. 95-101.
10. Blaine, J., and R. Burlot, "Non-Destructive Testing of Asphaltic Concrete Using the Light Goodman Vibrator: Study of the Influence of Temperature on the Viscoelastic Properties of the Material," *Journal of the Association of Asphalt Paving Technologists*, Vol. 39, 1970.

11. Dos Reis, H. L. M., Habboub, A. K., and S. H. Carpenter, "Nondestructive Evaluation of Complex Moduli in Asphalt Concrete with an Energy Approach," *Transportation Research Record 1681*, 1999, pp. 170-178.
12. Hochuli, A. S., Sayir, M. B., Poulidakos, L. D., and M. N. Partl, "Measuring the Complex Modulus of Asphalt Mixtures by Structural Wave Propagation," *Journal of the Association of Asphalt Paving Technologists*, Vol. 70, 2001.
13. Ferry, J.D., *Viscoelastic Properties of Polymers*, John Wiley, New York, 1980.
14. Williams, M. L., Landel, R. F., and Ferry, J. D., "The Temperature Dependence of Relaxation Mechanism in Amorphous Polymers and Other Glass-Liquids," *J. of Am. Chem. Soc.*, Vol. 77, 1955, p. 370.
15. 2002 Design Guide Draft – 2.4 Modulus of Elasticity for Major Material Groups, NCHRP Project 1-37A.
16. Pellinen, T. K., and M. W. Witzak, "Stress Dependent Master Curve Construction for Dynamic (Complex) Modulus," *Journal of the Association of Asphalt Paving Technologists*, Vol. 71, 2002.
17. Daniel, J. S., Kim, Y. R., and H. J. Lee, "Effects of Aging on Viscoelastic Properties of Asphalt-Aggregate Mixtures," *Transportation Research Record 1630*, 1998, pp. 21-27.
18. Lee, H. J., and Y. R. Kim, "Viscoelastic Constitutive Model for Asphalt Concrete under Cyclic Loading," *Journal of Engineering Mechanics*, ASCE, Vol. 124, No. 1, 1998, pp. 32-40.
19. Witzak, M. W., Bonaquist, R., Von Quintus, H., and K. Kaloush, "Specimen Geometry and Aggregate Size Effects in Uniaxial Compression and Constant Height Shear Tests," *Proceedings, Association of Asphalt Paving Technologists*, Vol. 69, 2000, pp. 733-793.
20. Chehab, G. R., O'Quinn, E., and Y. R. Kim, "Specim Geometry Study for Direct Tension Test Based on Mechanical Tests and Air Void Variation in SGC-Compacted Asphalt Concrete Specimens," *Transportation Research Record 1723*, 2000, pp. 125-132.
21. Witzak, M. W., and O. A. Fonseca, "Revised Predictive Model for Dynamic (Complex) Modulus of Asphalt Mixtures," *Transportation Research Record 1540*, 1996, pp. 15-23.
22. Pellinen, T. K., and M. W. Witzak, "Use of Stiffness of Hot-Mix Asphalt as a Simple Performance Test," Transportation Research Board (TRB) 2002 Annual Meeting, Washington, D.C.

23. Witczak, M. W., Pellinen, T. K., and M. M. El-Basyouny, "Pursuit of the Simple Performance Test for Asphalt Concrete Fracture/Cracking," Association of Asphalt Paving Technologists (AAPT) 2002 Annual Meeting, Colorado Springs, CO.
24. Witczak, M. W., Kaloush, K. E., and H. Von Quintus, "Pursuit of the Simple Performance Test for Asphalt Mixture Rutting," Association of Asphalt Paving Technologists (AAPT) 2002 Symposium, Colorado Springs, CO.
25. NCHRP Project 9-19, Draft Test Protocol A1: Dynamic Modulus of Asphalt Concrete Mixtures and Master Curves.
26. Chapra, S. C., and R. P. Canale, *Numerical Methods for Engineers*, 4th Edition, McGraw-Hill, Boston, 2002.